Dual Coolant Blanket Concept

Compiled by: S. Malang, K. Schleisiek
Contributors: L. Barleon, H. U. Borgstedt, L. Bühler,
F. Dammel, H. Feuerstein, A. Fiege, U. Fischer, H. Gerhardt,
H. Glasbrenner, T. Jordan, K. Kleefeldt, W. Kramer,
A. Möslang, P. Norajitra, G. Reimann, J. Reimann,
H. Reiser, H. Riesch-Oppermann, G. Schmitz,
H. Schnauder, R. Stieglitz, H. Tsige-Tamirat

Association KfK-Euratom
Projekt Kernfusion

Kernforschungszentrum Karlsruhe

KERNFORSCHUNGSZENTRUM KARLSRUHE

Association KfK - Euratom
Projekt Kernfusion

KfK 5424

Dual Coolant Blanket Concept

Compiled by: S. Malang, K. Schleisiek

Contributors: L. Barleon, H.U. Borgstedt, L. Bühler, F. Dammel, H. Feuerstein,
A. Fiege, U. Fischer, H. Gerhardt, H. Glasbrenner, T. Jordan, K. Kleefeldt,
W. Kramer, A. Möslang, P. Norajitra, G. Reimann, J. Reimann, H. Reiser,
H. Riesch-Oppermann, G. Schmitz, H. Schnauder, R. Stieglitz, H. Tsige-Tamirat

Kernforschungszentrum Karlsruhe GmbH, Karlsruhe

Dual Coolant Blanket Concept

– Summary of KfK 5424 –

S. Malang

Kernforschungszentrum Karlsruhe

Introduction

The Dual Coolant Blanket Concept is one of the four fusion DEMO blanket concepts under development in the European Union (EU). It has in common with a water-cooled liquid metal blanket the use of an eutectic lead-lithium alloy (Pb-17Li) as breeder material. The main advantages of liquid metal breeder materials compared to solid breeders are their higher thermal conductivity, the potential for tritium self-sufficiency without beryllium neutron multiplier, the immunity to irradiation damage and the possibility to extract tritium outside the blanket. The liquid metal breeder can be cooled either by water or helium, or can be circulated for external heat extraction ("self-cooled blanket"). Self-cooled blankets are in principle the most simple concepts, characterized by a small number of large ducts inside the blanket segments and the arrangement of the large heat transfer surface outside the irradiation environment which increases the reliability. The main challenge in designing self-cooled blankets is the strong influence of the magnetic field on the liquid metal flow. Especially the cooling of the first wall (FW) by liquid metal can cause high magnetohydrodynamic (MHD) pressure drops and implies the risk of a liquid metal spill since there is only a single wall between liquid metal and plasma. For these reasons a Dual Coolant Blanket Concept has been selected with a self-cooled breeding zone but a helium-cooled FW providing a double containment of the liquid metal. This concept and the main results of the R&D work carried out during its development are described in the report.

Blanket Design

A perspective view of an outboard segment is shown in Fig. 1. The helium-cooled FW and the helium manifolds at the rear side of the segment form a box containing the liquid metal breeder. This box is subdivided by stiffening plates into a number of ducts with liquid metal downflow in the rear three rows and upflow in the front row.
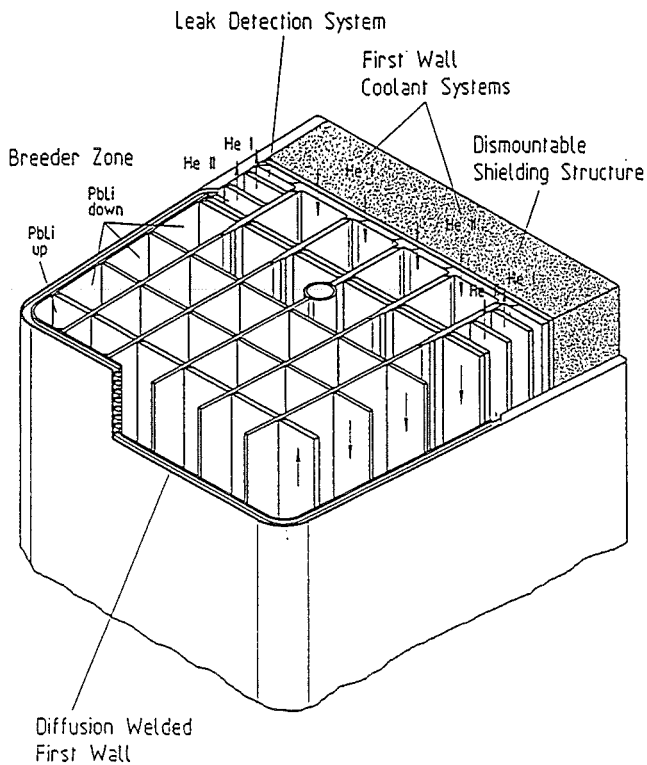
Fig. 1 Outboard blanket segment

The FW is manufactured by diffusion welding and bending and then the segment is assembled in poloidal direction by Electron Beam (EB) welding of sections with a height of about 1 m. There is a dismountable shielding structure with a separate cooling system attached to the breeding zone which can be reused after a blanket exchange in order to minimize waste disposal. A self-cooled breeding zone requires electrical insulation between the blanket structure and the flowing liquid metal. For this purpose the surface of the liquid metal channels are coated with a thin layer of aluminum oxide.

Neutronics

Subjects of the analysis are tritium breeding, nuclear power generation, shielding and activation. A tritium breeding ratio of 1.09 including the effect of 10 large radial ports has been determined which proves that liquid metal breeder blankets are feasible without beryllium neutron multiplier. An activation analysis of both structural material and liquid metal breeder including characteristic impurities provided the input for the safety analysis. Main emphasis has been placed on the generation of ^{210}Po which was previously regarded as one of the key safety issues of Pb-17Li blankets. The detailed analysis showed that the polonium generation is lower by orders of magnitudes compared to previous assessments.

Magnetohydrodynamics

An assessment of the minimum requirements on electrically insulating coatings showed that there is a margin of six orders of magnitude for the Radiation Induced Electrical Degradation (RIED) for a 10 μm thick alumina layer. However, a self-healing mechanism is required if cracking or flaking of the coating cannot be avoided. With such a layer the

maximum MHD pressure drop in the blanket is below 0.5 MPa and the flow distribution can be predicted with sufficient accuracy.

Thermal mechanical analysis

The inlet/outlet temperatures have been set to 275/425 °C for the liquid metal and to 250/350 °C for the helium with a gas pressure of 8 MPa. All calculated temperatures and stresses are below given engineering limits for MANET which have been specified for all blanket concepts. The strong segment box has a large margin for additional loads, e.g. caused by plasma disruptions and could tolerate an increase of the liquid metal pressure up to 8 MPa in case of large leaks between helium and Pb-17Li systems.

Systems for heat and tritium extraction

About 75 % of the total heat are extracted by liquid metal and 25 % by helium. Double-walled tubes are proposed for the steam generator in the Pb-17Li loops with the liquid metal flowing around the outer tubes, water (steam) in the inner tubes and NaK in the gap between the concentric tubes. Tritium permeates through the outer wall into the slowly flowing NaK where it is removed from by cold trapping. Experimental investigations of the loading and regeneration of such cold traps proved that this method meets the requirements with respect to low tritium inventory and acceptable permeation losses.
The technology of the helium loops including tritium extraction is investigated in the frame of the solid breeder blanket development.

Liquid metal and helium cooling loops are completely independent but deliver the heat to the same steam cycle. A steam cycle with a saturated steam turbine with about the same parameters as used in fission water reactors is proposed. A slight increase of the efficiency would be possible by superheating the steam with the liquid metal.

Reliability and safety

A high level of reliability and safety was the main incentive for the development of the Dual Coolant Blanket Concept. This concept is characterized by a leak tolerant design and a double containment of the liquid metal. The analysis based on data from fission reactors indicates that an availability of the entire blanket system including the external loops of more than 90 % can be achieved. This is mainly due to the arrangement of the heat transfer surface outside the blanket segments with the possibility to provide redundancy. An important safety feature is the use of three independent cooling systems for each segment (one liquid metal, two helium systems), resulting in a short temperature in-

crease only of less than 100 K during a LOCA with delayed plasma shutdown and in reliable after heat removal.

The total tritium inventory in the blanket system is below 50 g excluding the NaK-cold traps. The cold traps are regenerated batchwise at least twice a day and have a tritium inventory below 5 g each.

Experiments showing that polonium forms an intermetallic compound in Pb-17Li with a vapor pressure orders of magnitudes lower than that one for pure polonium lead together with the lower polonium generation to the conclusion that the α-emitter ^{210}Po is no longer a feasibility issue of lead-lithium blankets.

Remaining feasibility issues

Most of the critical issues of the blanket concepts have been investigated in sufficient depth to enable a profound assessment. The remaining open questions are mostly related to the behaviour under irradiation. A common issue of both liquid metal breeder blankets is the coating of the structural material required either as tritium permeation barrier in water-cooled blankets or as electrical insulator in self-cooled concepts. For both purposes an alumina layer with an aluminium-rich sublayer is envisaged. The fabrication technology of such duplex layers and their long-term performance under irradiation have to be investigated further.

Conclusions

The Dual Coolant Concept enables a simple design and has the potential for high safety and reliability. Tritium self-sufficiency can be achieved without a beryllium multiplier. Temperatures and stresses are well within acceptable engineering limits. The proposed tritium extraction method results in a low tritium inventory and tolerable permeation losses. ^{210}Po is not any more a feasibility issue. Manufacturing of the blanket segments is relatively simple and can be accomplished with near term technology.

The remaining feasibility issue is the performance of the insulating coating. The fabrication technology of this coating is a common issue with other blanket concepts needing a similar layer as tritium permeation barrier. Of special importance for the Dual Coolant Concept is the investigation of the radiation induced electrical degradation which requires further irradiation tests in the KfK Dual Beam Test Facility as well as in the HfR (Petten).

Abstract

A self-cooled liquid metal breeder blanket with helium-cooled first wall ("Dual Coolant Blanket Concept") for a fusion DEMO reactor is described. This is one of the four blanket concepts under development in the frame of the European fusion technology program with the aim to select in 1995 the two most promising ones for further development.

Described are the design of the blankets including the ancillary loop system and the results of the theoretical and experimental work in the fields of neutronics, magnetohydrodynamics, thermohydraulics, mechanical stresses, compatibility and purification of lead-lithium, tritium control, safety, reliability, and electrically insulating coatings. The remaining open questions and the required R+D programme are identified.

Dual Coolant Blanket Konzept

Zusammenfassung

Ein selbstgekühltes Flüssigmetall-Blanket mit heliumgekühlter erster Wand ("Dual Coolant Blanket Konzept") für einen Fusions DEMO Reaktor ist beschrieben. Dies ist eines der vier Blanket-Konzepte, welche im Rahmen des europäischen Fusions Technologie Programms entwickelt werden mit dem Ziel, in 1995 die zwei aussichtsreichsten Konzepte für die weitere Entwicklung auszuwählen.

Beschrieben sind das Blanket Design einschließlich der externen Kreisläufe und die Ergebnisse der theoretischen und experimentellen Arbeiten auf den Gebieten Neutronik, Magnetohydrodynamik, Thermohydraulik, mechanische Spannungen, Verträglichkeit und Reinigung von Blei-Lithium, Tritium-Extraktion und -Permeation, Sicherheit, Zuverlässigkeit und elektrisch isolierende Schichten. Die verbleibenden offenen Fragen und das erforderliche F+E Programm werden dargestellt.

Table of Contents

1. Introduction

The European Union (EU) is engaged since 1989 in a programme to develop tritium breeding blankets for application in fusion power reactors to be tested in the next step fusion reactor, presumably the "International Thermonuclear Experimental Reactor (ITER)" [1].

Four candidate blanket concepts are being developed within the framework of this programme with the intention to perform an independent assessment in 1995 in order to select the two most promising concepts. Two of these concepts rely on the use of lithium ceramics as breeder material, helium as coolant and beryllium as neutron multiplier. The other two concepts have in common the use of an eutectic lead-lithium alloy Pb-17Li as breeder material.

The main advantages of liquid metal breeder materials compared to solid breeder materials are their higher thermal conductivity, the potential for tritium self sufficiency without beryllium neutron multiplier, the immunity to irradiation damages, and the possibility to extract tritium outside the blanket. The liquid metal can serve either as breeder only, cooled by helium or water [2], or as breeder and coolant at the same time ("self-cooled blanket") [3], circulated to the external heat exchanger for heat removal. One interesting aspect of self-cooled blankets is the arrangement of the large heat transfer surface required in all blanket concepts at a location outside the blanket segment which increases the reliability since there is no need for kilometers of tubes with a large number of welds in the irradiation environment of a blanket segment without the possibility of providing redundancy.

The design of self-cooled blankets, however, has to overcome the following critical issues:

-       First wall (FW) cooling with liquid metal requires high velocities which can lead to high magnetohydrodynamic (MHD) pressure drops.

-       A single wall between the liquid metal and the plasma implies the risk of a liquid metal spill into the plasma chamber in case of leaks.

-       Malfunctions in the liquid metal circulation loop could make it difficult to maintain the breeder material liquid and to remove the decay heat.

These issues were the incentive to develop a blanket concept with a self-cooled breeding zone but a helium-cooled first wall [4].

This Dual Coolant concept is based on the following design principles:

●   First priority on safety and reliability, i.e.
  -   Double containment of the liquid metal breeder in a strong segment box,

- Leak tolerant design where a single leak in any of the welds does not require an immediate shut-down and blanket exchange,
- Redundant cooling systems ensuring reliable afterheat removal.

- Simple design and manufacturing
  - Large liquid metal ducts with a minimum of welds and low requirements with regard to the precision of manufacturing,
  - MHD pressure drop minimized by electrically insulating coatings,
  - Integrated manifold system for FW cooling.

- Waste generation minimized by separating the blanket structure to be disposed of from the shield which is reusuable after blanket exchange.

The main disadvantage of this Dual Coolant concept compared to the previously studied version of a self-cooled lead-lithium blanket concept [3] is the need for two completely different cooling systems. The two coolants - lead-lithium and helium - require completely different methods and components for heat and tritium extraction which increases the development cost, the space requirements and the operating complexity. A trade-off between these additional requirements and the improved safety and reliability features of the dual coolant concept led at this time to the selection of the dual coolant blanket concept as candidate for the European blanket selection to be compared with a water-cooled lead-lithium blanket concept and two solid breeder blanket concepts with helium cooling. This decision, however, should not exclude the development of entirely self-cooled blankets, especially if MHD-tests confirm a large heat transfer enhancement by a special kind of turbulence in simple poloidal ducts as indicated in recent tests [5,6].

2. Blanket Design

No detailed design of the candidate blanket concepts is required, but the conceptual design and the accompanying R&D work have to provide the basis for a meaningful selection.

2.1 DEMO Specification

The common basis for the blanket selection process is a DEMO-reactor specified by a Test Blanket Advisory Group (TAG). This specification is not the result of a detailed reactor study but a set of boundary conditions and minimum requirements for breeding blankets. Table 2.1-1 [1] shows the main parameters of DEMO, largely derived from NET (Next European Torus).

Table 2.1-1   Selected DEMO specifications

Major radius [m]	6.3
Minor radius [m]	1.82
Aspect ratio	3.45
Plasma current [MA]	20
Fusion power [MW]	2200
Average neutron wall loading [MW/m^2]	2.2
Average surface heat flux [MW/m^2]	0.4
Operating mode	continuous
Impurity control	double-null divertor
First wall protection	none
Number of TF coils	16
Toroidal magnetic field on axis [T]	6
Number of segments	32 inboard, 48 outboard
Blanket/shield thickness [m]	1.18 (inboard), 1.86 (outboard)
Structural material	MANET

The minimum requirements specified for all blanket concepts are:

-   tritium self-sufficiency (taking into account 10 horizontal ports of 3 m height and 1 m width)

-   full power life-time 20000 h, resulting in 70 dpa maximum first wall damage.

-   coolant conditions sufficient for electricity generation with a thermal efficiency $\eta \geq 30$ % where η is defined as the ratio between the electricity production from the blankets to the sum of neutron power and surface heat flux to the blankets.

-   blanket resistance to a major plasma disruption (current decay from 20 MA to zero in 20 ms) such that segments may become inoperative but still be removable by standard exchange procedures.

-   thermal and mechanical loads acceptable for the martensitic steel MANET.

2.2   Design Description

The overall geometry of the blanket segments is a part of the DEMO specification. A vertical cross-section of the torus with the arrangement of the blanket segments and the access lines is shown in
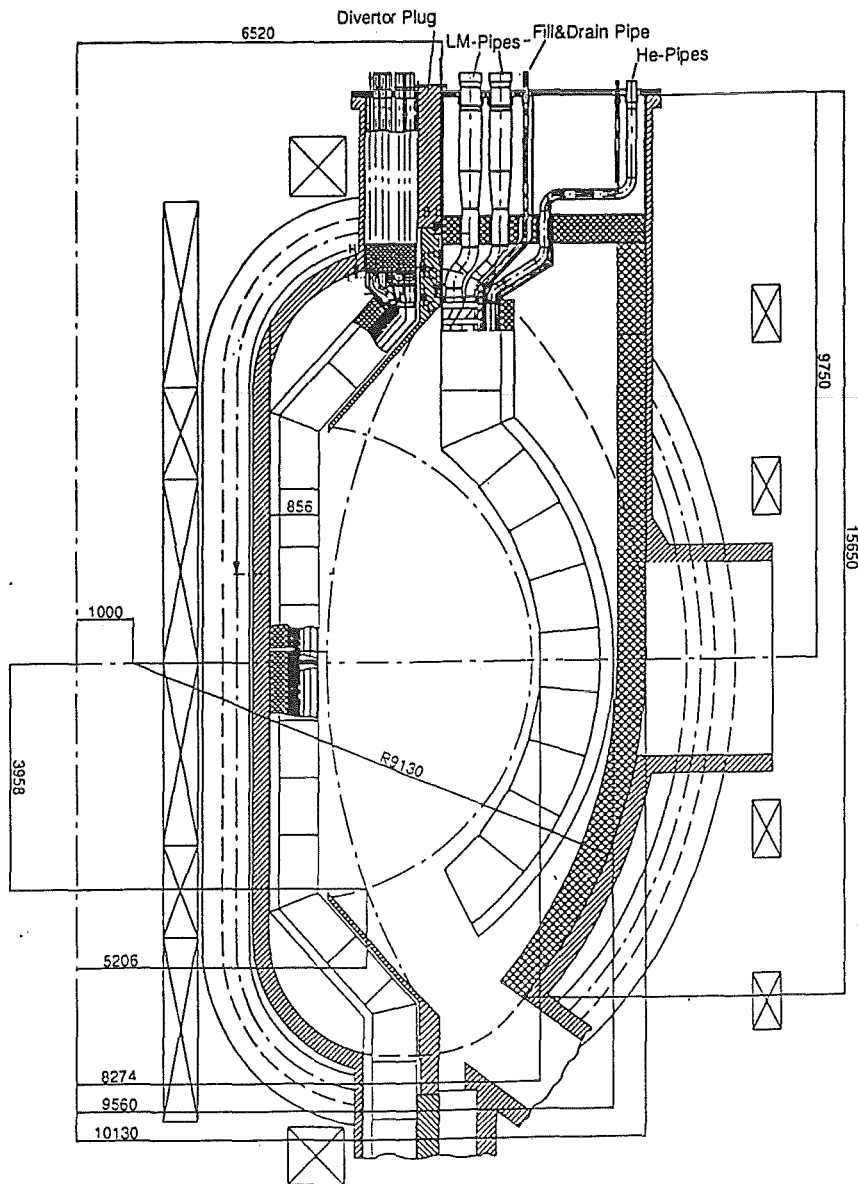
Fig. 2.2-1: Cross section of the DEMO reactor with Dual Coolant Blanket

Fig. 2.2-1. The specification allows for a design of the inboard segment split into two halves with the cooling lines for the lower half coming from the bottom of the torus. This is especially advantageous for liquid metal cooling which is more difficult for the inboard segment due to the higher magnetic field and the more restricted space in this region. Splitting of the inboard segment halves the mass flow and the duct length, respectively, leading to a reduction of the MHD pressure drop by roughly a factor of four at the expense of doubling the number of supply lines. The resulting pressure drop for a divided inboard segment is smaller than for an undivided outboard segment. Therefore, this solution has been selected as the reference design. Undivided inboard segments, however, would be feasible too, since the MHD pressure drop is decisively reduced by insulating coatings in all liquid metal ducts.

The torus is divided in the toroidal direction into 16 sectors. Each sector contains 3 outboard and 2 inboard segments which are exchanged through a common port at the top of the torus. All access lines for the 3 outboard segments and the upper halves of the inboard segments enter the vacuum chamber through this port. Only the lower halves of the two inboard segments are served from the bottom together with the lower divertor plates.

Each blanket segment is connected to one liquid-metal loop and to two completely separated helium cooling loops. The arrangement of the cooling lines for liquid metal and helium in the region of the port is shown in Fig. 2.2-2.
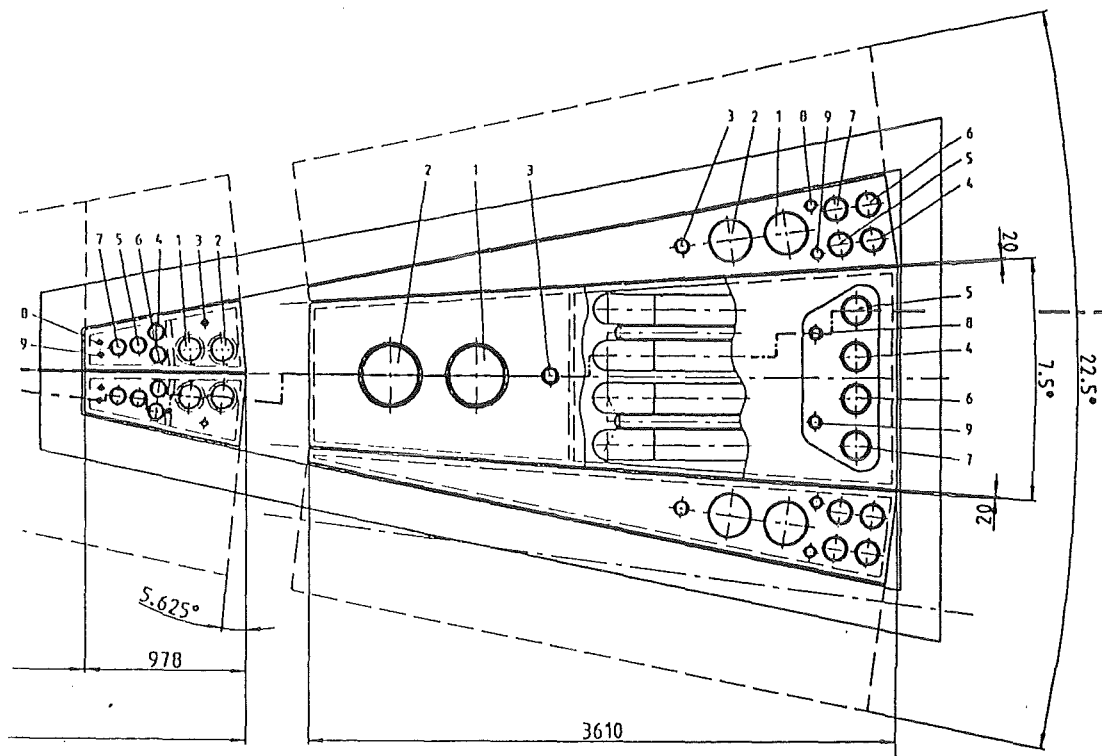
1	liquid metal inlet	4	helium I inlet
2	liquid metal outlet	5	helium I outlet
3	liquid metal filling/draining	6	helium II inlet
8, 9	leak detection	7	helium II outlet

Fig. 2.2-2: Top view of the flange covering blanket exchange port

Figure 2.2-3 shows a perspective view of an outboard segment. The concept is characterized by a U-shaped first wall with helium cooling channels in radial/toroidal direction. This FW forms together with the helium manifolds at the back side of the segment a box containing the liquid metal breeder. There is a grid of steel plates inside this box creating large liquid metal ducts and, as an additional function, reinforcing the FW box. Horizontal cross-sections of outboard and inboard segments are shown in Fig. 2.2-4.
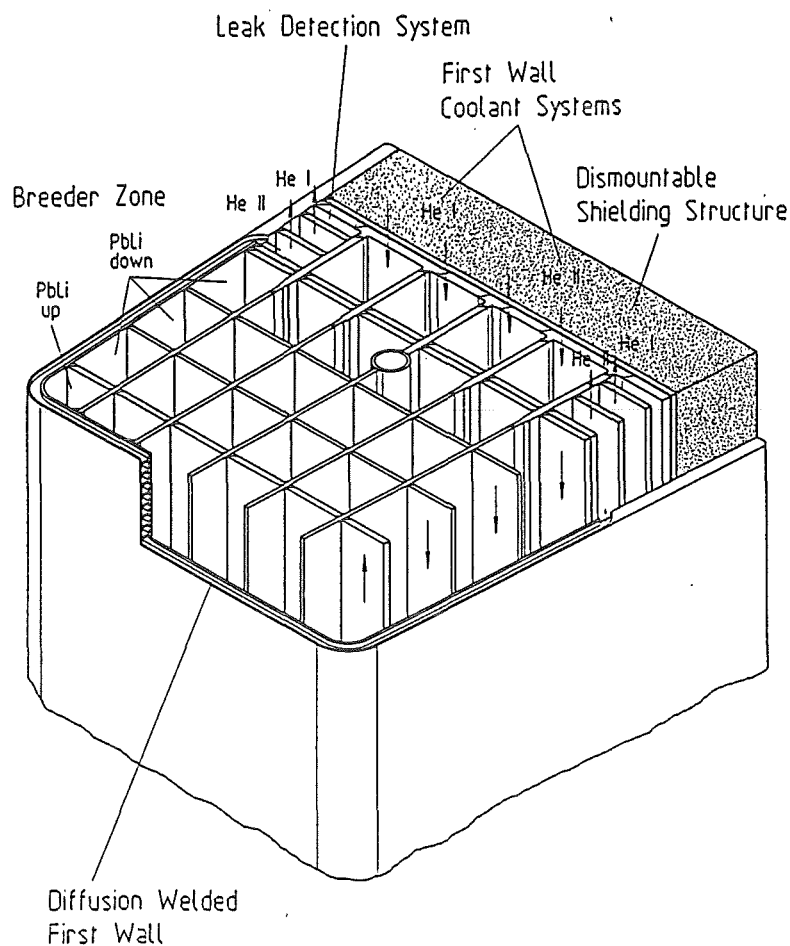
Fig. 2.2-3: Perspective view of an outboard segment

The Pb-17Li enters the blanket at the top, flows downwards in the three rows of parallel channels at the rear side, turns around at the bottom by 180°, and flows upwards in the first row. This allows to adjust the velocity in each row according to the local heat generation rate. Compared to an entirely self-cooled concept, the liquid metal ducts are larger and the required liquid metal velocity is smaller since only the internally generated heat has to be removed by liquid metal cooling. Nevertheless, electrical insulation is required between the load-carrying walls and the flowing liquid metal. This could be achieved either by the use of flow-channel inserts in which a thin ceramic layer is sandwiched between two steel sheets or by coating of the duct walls with an insulating layer. The second method is the proposed solution although the feasibility has not yet been demonstrated.

A blanket segment is constructed by welding together sections of the U-shaped box with a height of approximately 1 m. The sections are fabricated by diffusion welding and subsequent bending of two straight plates containing the milled cooling channels. The design and technology of the welds between sections are important details of the concept. It is foreseen to use electron beam welding to

a) outboard   b) inboard
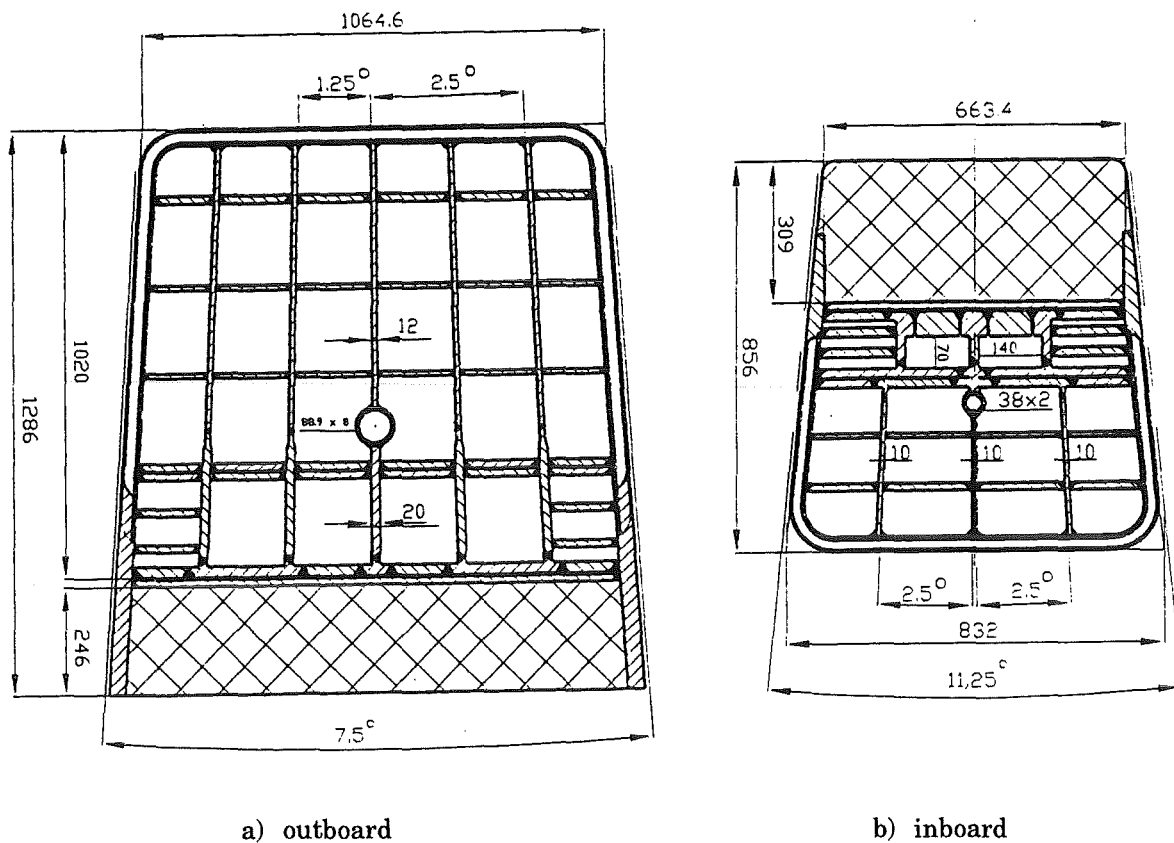
Fig. 2.2-4: Horizontal cross section of blanket segments

obtain two independent welds with a monitoring gap in between (see Fig. 2.2-5). The same design principle is employed throughout the blanket segment as a barrier between liquid metal and vacuum and ensures a real double containment of the liquid metal. Between helium and plasma a single wall is allowed, but only when there is no weld at this wall. For details see Sect. 2.3.

Helium cooling of the FW is divided into two completely independent systems. The cooling channels are alternatively connected to one of the systems in order to minimize FW temperature increase in case of a Loss-Of-Coolant Accident (LOCA) in one of the circuits.

The selected design of the FW cooling is characterized by the following features:

a)   Integrated manifolds

     The helium manifolds are an integral part of the segment box as shown in Figures 2.2-3 and 2.2-4. No separate welds for each cooling channel with all the implications in regard to manufacturing and reliability are required.
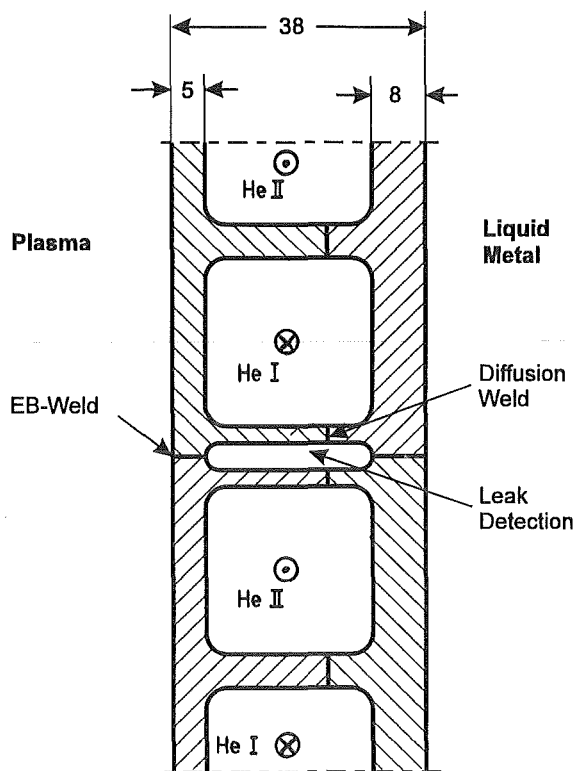
Fig. 2.2-5: FW cooling channels and connection between FW sections
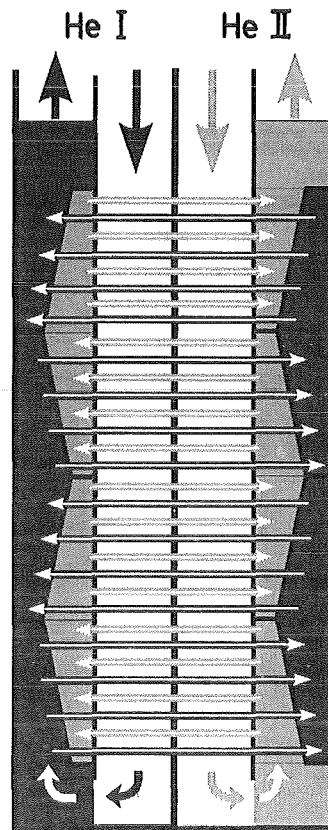
Fig. 2.2-6: Helium flow in FW and manifolds

b) Multiple passes of the coolant through the FW

The total helium mass flow passes 4 times through the FW in the outboard and inboard segment. This allows for relatively large coolant channels leading to a very stiff segment box and results in a small temperature rise for each pass.

c) Reduction of the number of parallel channels per pass with increasing distance from the blanket inlet.

This increases the helium velocity and consequently, the heat transfer coefficients in blanket regions with higher helium temperatures.

d) Alternating flow direction in the FW cooling channels

The helium of the two cooling loops flows in opposite direction through the FW cooling channels. This leads to a symmetric temperature field in the segment box with lower thermal stresses.

e) Heat transfer at the FW wall enhanced by surface roughening

The envisaged manufacturing method allows artificial surface roughening at the FW in order to enhance the heat transfer at the wall with the high heat flux. Since only one of four walls in a channel is roughened, the increase in pressure drop is marginal. This method results in lower structural temperature and smaller temperature variations in the segment box.

The helium flow in the manifold and the distribution to the cooling channels are shown in Fig. 2.2-6. Helium enters the segment in two parallel channels at the top, flows downward at the rear side of the segment and turns around at the bottom by 180°. The manifolds in upward direction are divided into two parallel ducts with varying cross-sections to account for the variation of the helium flow. The results of this geometry are the desired flow scheme in the FW channels and a roughly constant velocity in the manifolds.

An important design issue of breeding blankets for a power reactor is shielding of the superconducting magnets. The blankets have to reduce both neutron and gamma fluxes by a large degree since the additional shielding components including the vacuum vessel cannot be replaced during the entire reactor life-time. It is clear that the blanket itself has to be replaced 5 to 10 times during this time due to the neutron damage of the first wall. The neutron damage in the blanket, however, decreases exponentially in radial direction and would allow to split the blanket in a front part to be replaced and disposed of quite frequently and a rear part which could be a reusable component. Hence, the design presented attempts to minimize the waste generation by designing the shielding zone as a dismountable component with separate cooling. The neutron flux in this region is low enough to allow a reuse over the entire reactor life-time. This shield containing roughly twice as much steel than the front part has the additional benefit of providing a strong mechanical support for the blanket structure.

2.3   Fabrication and Assembly

Fabrication and assembly of the blanket segments have been investigated in collaboration with several industry companies and research organizations [7]. The principal results are described subsequently.

The first fabrication step is the milling of the grooves forming the FW cooling channels and the bonding of the two plates by diffusion welding. A first series of bonding tests was performed involving small MANET specimens (80 mm in diameter) with cooling and leak detection channels to determine the optimum parameters for the preparation of the surfaces to be joined and for pressure and temperature. After heat treatment of the bonded specimens a leak test was carried out at 10 bar internal pressure and, in addition, metallographic investigations and bending tests were performed with specimens made of bonded material and - for comparison - with those made of the

base material. All specimens were found to be tight. The best bonding results have been obtained for specimens with finely ground surfaces (roughness ≤ 3 µm) and bonding temperatures of 980 °C and 1050 °C, respectively. The pressure applied during bonding was 30 MPa and 18 MPa, respectively, for one hour and thereafter 7 MPa. Bending tests with these specimens showed that the strength was nearly equivalent to that of the base material. In a second test series three MANET plates, 320 mm in diameter, with a cooling channel geometry typical of the first wall, were bonded. Subsequent leak tests at 80 bar and 150 bar internal pressure provided evidence of tightness. The conclusion from these tests is that diffusion welding is an efficient method for the fabrication of first wall plates with integrated cooling channels.

The next important fabrication step is the bending of the FW plates to obtain the U-shape of the box. Bending angles of about 86° for the outboard and 96° for the inboard segments have to be realized. No major problems are expected in the bending process because a) the diffusion weld will be positioned in the neutral plane of the double plate, and b) there is no need for very small bending radii. Nevertheless, bending tests on representative FW plates have to be carried out and are scheduled for 1995.

The next step in the fabrication process is the preparation of the poloidal surfaces of FW sections including the milling of the leak detection channels, and the connection of the sections by electron beam (EB) welding. A development and qualification program is presently carried out with martensitic steel which includes the investigation of possibilities for weld inspection. In a first test series the optimum welding parameters have been determined. Both parts of the weld with the leak detection gap in between can be carried out in one step. In parallel ultrasonic (US) investigation was qualified as an efficient inspection method by comparing the results with those of X-ray inspection. The evaluation and documentation of these tests is still under way. Actually further welding specimens are being manufactured and inspected by US. Metallografic investigations of these specimens will be carried out and compared with the US inspection results to obtain a data base for the reliability of this kind of welds. In addition to the tests, numerical simulation of the EB-welding was performed using ABAQUS, and time-dependent stress- and temperature fields were obtained [8]. Results allow to predict the size of the heat affected zone and the welding stresses. The welding procedure of the U-shaped wall has still to be investigated. In particular it must be clarified whether the usual EB procedure, i.e. the movement of the workpiece, will be applied, or whether it is more efficient to move the EB gun around the workpiece. In any case, the necessary welding equipment including a vacuum chamber of suitable size must be realized. The EB welding technique will also be applied to join the lower bottom plate and the upper tube plate to the U-shaped FW segment.

In the next step the internal plates forming the Pb-17Li channels will be inserted and connected to the box by butt or fillet welds. These are mainly longitudinal welds which can be carried out with

automatic welding machines. The load of these welds under normal operating conditions is rather low. Furthermore, small failures and even minor leaks can be tolerated (see Sect. 7). Hence, it seems acceptable that full inspection of these welds may not be possible.

The next major operation is the assembling of the plates forming the helium manifolds at the backside of the blanket. For this step about the same welding and inspection conditions apply as for the plates inside the Pb-17Li zone. However, according to the requirement described in Sect. 2.2, the walls separating the helium channels from either the Pb-17Li or the vacuum have been designed as double containment with an intermediate gap connected to the leak detection system, and small leaks of a single weld will not entail the need to exchange immediately the blanket segment concerned. Hence, also here the limitations of inspectability of the welds during fabrication seems to be acceptable.

At the end of the box fabrication the whole assembly will be submitted to pressure and leak tests.

The design and assembly of the pipes between the upper tube plate of the segment and the flange of the port is a difficult task because of the space limitation. A preliminary design has been elaborated for the central outboard and the inboard segments (see Figs. 2.2-1 and 2.2-2). For the lateral outboard segments a similar solution could be applied as for the inboard segments. Further studies are necessary concerning the methods and tools required for the welding of the tubes.

A conceptual design has been developed for the detachable connection between the blanket segment and the reusable shield. The details of this concept have still to be worked out. The coating of the Pb-17Li channels providing the necessary electrical insulation is described in Sect. 8.

The insertion of the five segments of a blanket sector has to be carried out in the following order: inboard segments, lateral outboard segments, central outboard segment. The exchange of an inboard segment is only possible after the removal of the central and at least of one lateral outboard blanket. More detailed studies are necessary on the sequence of work, handling of components, methods to be used for pipe connection and separation, safety of the exchange procedure, and time periods needed for these operations.

A further subject to be investigated in more details is filling and draining of the segments with Pb-17Li. It is anticipated to heat up the blanket structure with the helium cooling loops and fill in the breeder material through the filling tubes leading to the bottom of the segments as shown in Figs. 2.2-1 to 2.2-4. The same tubes are used for draining the segments. In this case the liquid metal has to be pushed through these tubes by a suitable gas pressure applied through both the inlet and outlet ducts of the liquid breeder circulation loops.

2.4 Neutronics Analysis

The neutronics analysis is based on three-dimensional Monte Carlo calculations with the MCNP-code [9] and nuclear cross-section data from the European Fusion File EFF [10]. A geometrical model has been set up for half a 22.5 ° torus sector of the DEMO-reactor (1/32 of the torus) with one inboard and one and a half outboard segments. Reflecting boundary conditions are applied at the lateral walls of the modelled torus sector. The model includes the vacuum chamber, first wall and blanket segments, the vacuum vessel, top and bottom divertor as well as a bottom divertor exhaust chamber with a pumping duct entrance. Fig. 2.4-1 shows a radial-poloidal cross-section of the MCNP torus sector model.
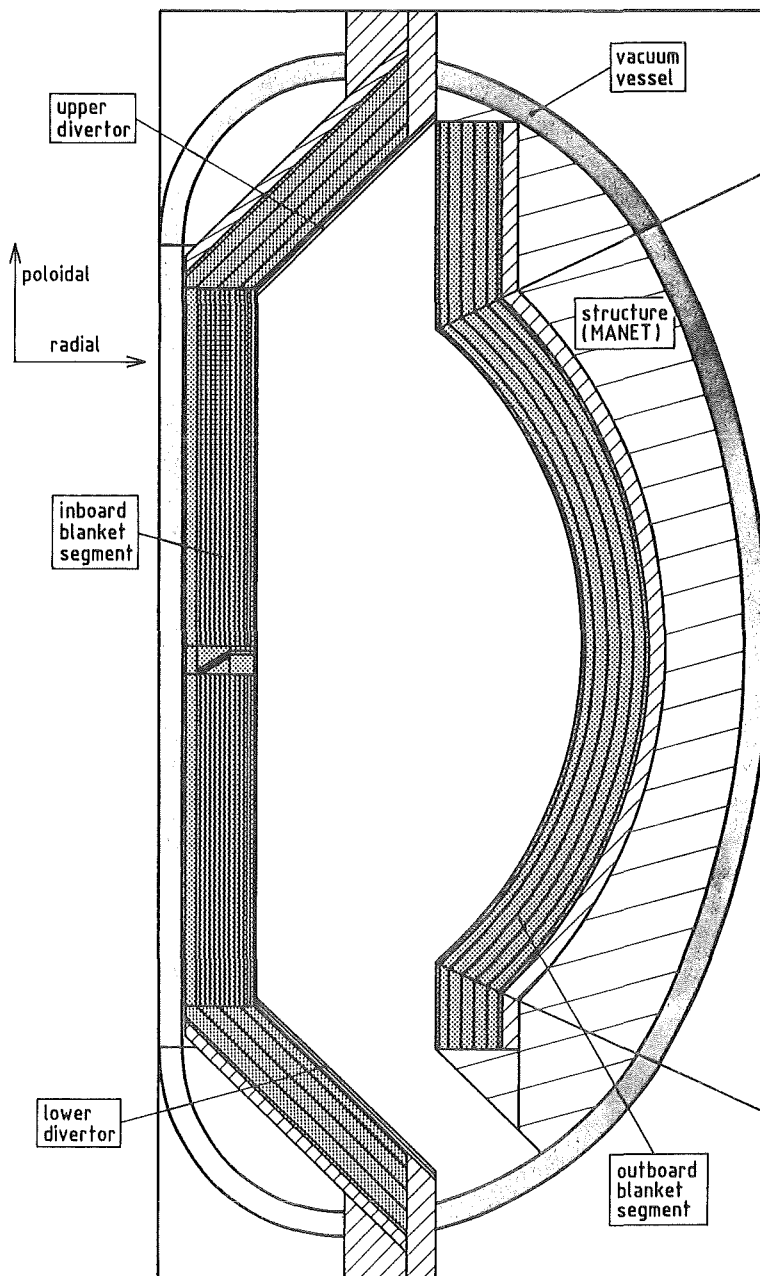
Fig. 2.4-1: Radial-poloidal cross section of the MCNP torus sector model

The spatial neutron source distribution is sampled in a special FORTRAN routine linked to the MCNP-code, for details see Ref. [11]. The following plasma parameters are used for the DEMO-reactor [3]: Major plasma radius = 630 cm, minor plasma radius = 182 cm, elongation = 2.17, excentricity = 16.2 cm, maximum triangularity = 0.57.

2.4.1 Tritium Breeding Ratio

For calculating the tritium breeding ratio (TBR) about 90,000 source neutron histories have been followed in the Monte Carlo calculation. A ^{6}Li-enrichment of 90 at% is assumed for the Pb-17Li liquid metal breeder. The total radial thickness of the liquid metal channels amounts to about 30 cm inboard and 68 cm outboard. In addition, the divertor region is utilised for breeding. Table 2.4-1 shows the neutron balance and the associated statistical errors obtained for the TBR-calculation.

Tritium breeding will be affected by the presence of blanket ports for plasma heating, remote handling, pellet injection, diagnostics etc.. Ten horizontal ports centred at the equatorial plane of the outboard blanket segments are foreseen for the DEMO-reactor. Each blanket port covers an area of 340 cm height times the full segment width. The impact on the breeding performance of both liquid metal and solid breeder blankets has been assessed previously [12]. Based on these results, the global TBR is expected to decrease to about TBR = 1.09 in the presence of ten ports.

Table 2.4-1   Neutron balance

Neutron multiplication	1.59 ± 0.1%
Tritium breeding ratio	
Outboard blanket segment	0.82 ± 0.3%
Inboard blanket segment	0.23 ± 0.5%
Divertor breeding region	0.10 ± 0.9%
Total tritium breeding ratio	1.15 ± 0.2%

2.4.2 Power Generation

For calculating the nuclear power generation a coupled neutron-photon Monte Carlo transport calculation has been performed. About 350,000 source neutron histories were followed in this calculation. The normalisation was performed for a fusion power of 2200 MW. Table 2.4-2 shows the resulting power generated in the inboard and outboard blanket segment. In the DEMO-reactor, equipped with 32 inboard and 48 outboard blanket segments, a total power of 1806 MW would be obtained.

Table 2.4-2   Power generation [MW] in the blanket segments
(2200 MW fusion power)

Outboard blanket segment (7.5°)	26.7
Inboard blanket segment (11.25°)	
Central part	12.9
Divertor breeding region	3.5
Total inboard	16.4

A fine radial-poloidal segmentation scheme has been introduced in the Monte Carlo calculation to obtain the spatial power density distribution in the blanket segments. Each liquid metal channel was split into radial segments with thicknesses between 3 and 5 cm. The outboard blanket was split into 18 poloidal segments of 5° with respect to the centre of the poloidal curvature located at $R = 340$ cm in the equatorial plane. At the inboard side the upper half of the blanket segment was split into 10 poloidal segments with a poloidal height of about 40 cm each.

The radial and poloidal profiles of the power density are comparatively flat due to the inherent nuclear properties of Pb-17Li and the absence of any neutron moderator. At the outboard side the peak power density for Pb-17Li is 19.4 MW/m^3 (equatorial plane), at the inboard side 17.1 MW/m^3. The poloidally averaged values are 16.6 and 12.3 MW/m^3, outboard and inboard, respectively. For the MANET of the first wall (5mm thickness) the peak values are 23.9 and 20.3 MW/m^3, the poloidally averaged ones 20.7 and 15.2 MW/m^3, outboard and inboard, respectively.

2.4.3 Afterheat Generation

A detailed analysis of the afterheat generation has been performed for the outboard blanket segment [13] by combining three-dimensional Monte Carlo transport calculations with the MCNP-code and afterheat calculations with the FISPACT [14] inventory code. Neutron spectra were calculated in 100 energy groups (GAM-II structure) in the first wall, the liquid metal channels, the steel walls in between, the rear wall and the steel back plate of the outboard blanket segment. About 300,000 source neutron histories were followed in the MCNP-calculation for the spectra to assure a sufficient statistical accuracy.

FISPACT inventory calculations were performed for each radial zone of the outboard blanket segment using the neutron spectra provided by the MCNP calculation both for the peak values at the equatorial plane and the poloidal average values. The cross-section data of the European Activation File EAF-2 [15] were used in the FISPACT calculations.

Table 2.4-3   After heat generation [MW] in the central outboard
               blanket segment at reactor shutdown (2200 MW fusion
               power, 20000 h of operation)

MANET	0.208
Pb-17Li	0.527
Total	0.735

Table 2.4-3 shows the total afterheat power calculated for the central outboard blanket segment at reactor shut down (t=0). An integral operation time of 20,000 hours at a fusion power 2200 MW is assumed in this calculation. The maximum afterheat power density at the equatorial plane amounts to 0.77 MW/m^3 for the MANET at the first wall (3.3 % of the direct heating) and to 0.64 MW/m^3 for Pb-17Li in the front liquid metal channel (2.9 % of the direct heating). The afterheat generation in Pb-17Li is decreasing fast (within 10 minutes to less than 0.02 MW/m^3) because it is dominated by the short-lived lead isotopes ^{204}Pb and ^{207}Pb. The decay heat generation for MANET is roughly constant over the time period of a few minutes after shutdown. According to the half life of the main contributor ^{56}Mn ($T_{1/2}$ = 2.58 h) it further decreases by one order of magnitude after one day.

2.4.4 Activation

For calculating the activation the method developed for the afterheat calculation has been followed. In the activation calculation it is mandatory to take into account material impurities and tramp elements to analyse their impact on the activation characteristics. The following impurities have been used for Pb-17Li [16]: 10 wppm Zn, 10 wppm Fe, 43 wppm Bi, 5 wppm Cd, 5 wppm Ag, 5 wppm Sn, 2 wppm Ni. The NET material specification [17] for MANET-1 was assumed in the activation calculation for the steel (in w%): 0.13 C, 0.35 Si, 1.0 Mn, 0.005 P, 0.004 S, 10.5 Cr, 0.85 Ni, 0.75 Mo, 0.20 V, 0.15 Nb, 0.03 N, 0.05 Al, 0.008 B, 0.02 Co, 0.02 Cu, 0.09 Zr. Numerical results of the activation analysis are given in Section 6. For more detailed results see Ref. [13]. Only some outstanding features are discussed in the following.

The activation behaviour of the MANET steel in the blanket is not significantly affected by the impurities. This holds for the activation inventory, the contact γ - dose rate and the radiological hazard potential. For Pb-17Li, on the other hand, both the contact γ - dose rate and the radiological hazard potential are affected by the impurities at cooling times larger than one year. This is mainly due to contributions from Ag activation products (^{108m,110m}Ag) and ^{60}Co resulting from the Ni activation.

The generation of the radiotoxine ^{210}Po in irradiated Pb-17Li has been studied previously [18]. It has been shown that the ^{210}Po activation inventory had been largely overestimated in the past

due to cross-section data uncertainties, deficiencies in the transport calculations, and uncertainties in the activation calculation due to the neglection of the liquid metal circulation. The latest results yield a ^{210}Po concentration of ≈ 0.2 appb.

2.4.5 Shielding Efficiency

The shielding performance of a breeding blanket in general is poor. This holds especially for the self-cooled Pb-17Li blanket due to the absence of any neutron moderating material. Sufficient shielding has to be provided by material components arranged between the toroidal field (TF) coil and the blanket: the vacuum vessel and the back of the blanket segment. At the inboard side radiation shielding is most crucial. There the totally available space amounts to 115 cm. The thickness of the vacuum vessel, acting as major shielding component, is 30 cm; 85 cm are left for the blanket segment. Actually only 37 cm need to be used for the breeding zone due to the good breeding performance of the Pb-17Li. Therefore, 48 cm of the blanket is available for additional shielding.

Detailed three-dimensional shielding calculations have been performed for the previous version of the self-cooled liquid metal blanket [3] . In that case the total depth of 85 cm was utilised for the inboard breeding blanket. It has been shown that the required radiation design limits for the TF-coil can be met for an integral operation time of 20,000 hours by applying different technical measures for improving the shielding efficiency, e. g. by optimising the vacuum vessel for shielding, or, by inserting an efficient neutron moderating material at low volume fractions (20% ZrH) into the blanket back part. In the actual design 48 cm of the breeding blanket can be utilised for shielding. In this case the required radiation design limits can be met for an integral operation time of 10 years provided that neutron moderating material (e. g. ZrH or water) is inserted into the additional shielding zone.

2.5 Magnetohydrodynamic Analyses

In self-cooled liquid metal blankets the interaction of the flowing liquid metal with the plasma confining magnetic field results in the induction of a voltage and in consequence electrical current flow. Electrical currents perpendicular to the magnetic field induce Lorentz forces opposing the fluid motion and leading to magnetohydrodynamic (MHD) pressure losses far above those in ordinary hydrodynamics. The magnitude of the currents determine the MHD pressure loss. When the current loop is closed by electrically conducting duct walls, the MHD pressure drop is proportional to the wall thickness. In electrically insulated ducts the currents have to short circuit within the fluid, which results in substantially lower pressure drops than in ducts with electrically conducting walls.

The design is based on duct walls covered with an insulating coating (see Sect. 8). As back-up solution, the use of flow channel inserts (FCI) is also considered in the MHD analyses. These FCIs

consist essentially of a sandwich of steel sheets with a ceramic layer in between and are fitted loosely in the duct.

For the purpose of analysis, the blanket has been divided into basic 2D- and 3D-hydraulic elements shown in Figure 2.5-1. For those elements, MHD analyses which are based both on experimental and theoretical work [3, 19 to 25], have been conducted at KfK in cooperation with the Argonne National Laboratory and the Physics Institute of the Latvian Academy of Science.
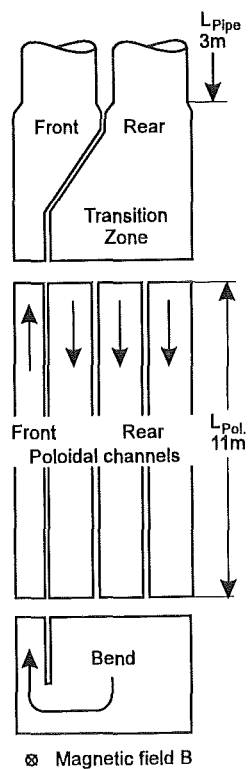
Fig. 2.5-1: Characteristic liquid metal flow geometries

The laminar MHD flow in most parts of the blanket (circular access tubes, rear and front poloidal ducts) is essentially two-dimensional and can be calculated rather accurate by using simple analytical correlations for insulating ducts as well as for ducts with thin conducting walls.

For the more complex situation of 3D MHD flows as in the transition zones of varying magnetic field, distributors, and 180°-turns, computational tools which are based on an inertialess model (Core Flow Approximation) have been developed. Experimentally, the validity of the codes has been verified and, additionally, the influence of inertia effects on the flow and the scaling laws of inertia effects have been determined.

Based on this knowledge the calculations of the pressure drop for both methods (insulated ducts, FCI-technique with a 0.5 mm thick steel liner) listed in Table 2.5-1 have been carried out for the outboard and the inboard blanket segments under the named conditions. Also the arrangement of

the blanket segments has to be taken into account. In the access tubes of the lateral outboard segments, which are hidden behind the toroidal field coils and therefore require a Z-shaped design, the pressure drop due to the bend and the fringing field in this region is relatively large.

Tab. 2.5-1   MHD pressure drop in MPa of the outboard and inboard blankets

	Insulated ducts		Ducts with FCI	
	Outboard	Inboard	Outboard	Inboard
Circular	0.236*	0.026	0.793*	0.24
Rear poloid.	0.012	0.006	0.72	0.42
Front poloid.	0.030	0.008	2.04	0.60
180°-turn + manifold	0.010	0.008	0.037	0.02
Inlet transition	0.052	0.038	0.05	0.04
Outlet transition	0.060	0.044	0.06	0.04
FCI overlapping	-	-	0.57	0.50
	0.400	0.130	4.26	1.86

*Central segment   0.036   0.34

Remarks to the two cases listed in Table 2.5-1:

a)   Insulated Ducts

The extremely low pressure drop in a blanket system with insulated duct walls offers the opportunity of an MHD throttling to stabilize the flow rates in the rear poloidal channels. Such a measure would mitigate the maldistribution if the electrical insulation would partly deteriorate.

A crucial issue is the quality of insulation required to achieve the low pressure drop present in MHD flows in insulated ducts. In numerical simulations [23] it turned out that the resistance of the insulation characterized by the product resisivity x layer thickness has to be at least 10^{-2} Ωm^2. This value requires for a 10 µm thick layer a resisivity of 10^3 Ωm which is at least six orders of magnitude lower than the resisivity of pure, unirradiated alumina at 450 °C.

b)   Thin conducting walls

The feasibility of the FCI-technique has been shown experimentally in [19]. An effect associated with the FCI-technique are 3D MHD flows due to the overlapping of the FCI´s in the

poloidal ducts. This effect of the overlapping has also been taken into account in the pressure drop assessment. Although the pressure drop is higher than in the insulated duct case, the resulting liquid metal pressure remains below the maximum tolerable value determined from material stress considerations. The pressure drop could be reduced by modifications of the duct geometries if the FCI-technique becomes the preferred option.

2.6 Thermal-mechanical Analysis

This section summarizes the results of the thermohydraulic layout of the blanket and of the calculations of the temperature and stress distribution. A general description of the cooling concept has already been given in Sect. 2.2. The spatial power density distribution needed for the thermal analysis is resulting from the neutronics analysis described in Sect. 2.4 and may be found in [26]. The maximum power density occurs in the poloidal mid-plane of the outboard blanket and amounts to 23.9 MW/m^3 in the structural material and 19.4 MW/m^3 in the Pb-17Li. For the plasma facing blanket surface an average heat flux of 0.4 MW/m^2 and a local peak value of 0.5 MW/m^2 was assumed.

The thermohydraulic layout and the calculation of the helium pressure drop are described in detail in [26]. The total power generated is 30 MW in an outboard segment and 9.6 MW in each inboard half-segment including surface heat load but without power in the shield. The inlet and outlet temperatures of the helium (250/350 °C) and the Pb-17Li (275/425 °C) have been selected using arguments like: sufficient margin to the DBTT of the martensitic steel and the melting point of the Pb-17Li, limitation of the maximum structural and Pb-17Li interface temperature, attractive thermal efficiency of electrical power generation, etc. The helium pressure is 8 MPa. The mass flow rates needed in the different systems and the local coolant temperatures were then calculated from energy balances with the additional assumption that the middle of the walls separating the helium and the Pb-17Li is an adiabatic limit.

After definition of the cooling systems the pressure drop of the helium flow was calculated. It amounts to 0.15 MPa in the outboard and 0.12 MPa in the inboard blankets. These values include the effect of the artificial surface roughness of one of the four walls of the FW cooling channels. The pressure drop of the Pb-17Li flow is discussed in Sect. 2.5.

For the calculation of the temperature and stress distribution in the structures, the FE code ABAQUS was used. The analysis was carried out for a radial/toroidal section of the outboard blanket with a poloidal height of one helium channel pitch (see Fig. 2.6-1). The 3-dimensional FE mesh was generated using the CAD system BRAVO3/GRAFEM. The Pb-17Li temperature was determined in a preliminary simulation assuming slug flow. The alternating directions of the helium flow in neighbouring channels were taken into account by an iterative adjustment of the poloidal interface temperatures. For the shield at the blanket back side a constant temperature of 285 °C
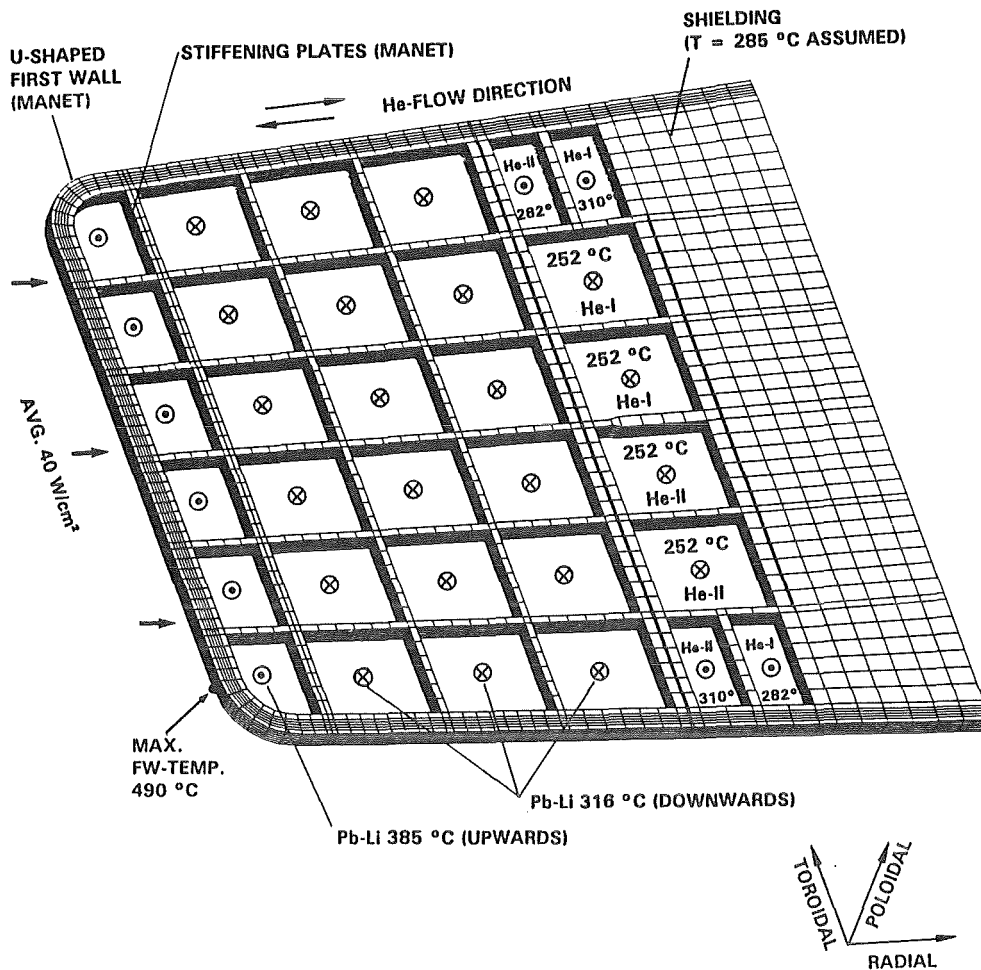
Fig. 2.6-1: FE mesh used in 3D ABAQUS calculation

was assumed. Fig. 2.6-2 (top) shows the calculated temperature for a surface heat load of 0.4 MW/m². The maximum temperature occurs at the edge of the plasma-facing surface of the blanket segment and amounts to 490 °C. At the peak thermal load of 0.5 MW/m² the maximum structural temperature reaches 520 °C.

In the stress calculations a quasi plane strain condition was applied for the poloidal surfaces of the model which means that these planes remain planar and parallel. For the breeder zone (Pb-17Li) the same pressure of 8 MPa was assumed as for the helium system. This is a conservative upper limit of the internal load which is reached only in case of a large leak between the helium and the Pb-17Li systems. The temperature field for 0.4 MW/m² surface heat flux was used. The calculated primary von Mises stress amounts to 120 MPA. This value is below the limits for yield, rupture and 20 000 h creep stress allowed for MANET at 490 °C according to ASME (1.5 x S_m = 217 MPa in the case of bending) [27, 28]. The total von Mises stress distribution is shown in Fig. 2.6-2 (bottom). The maximum stress occurs at the location of the temperature maximum and amounts to

TEMP.
(°C)
K 500
J 480
I 460
H 440
G 420
F 400
E 380
D 360
C 340
B 320
A 300

MAX.
FW-TEMP.
490 °C

VON MISES
(MPa)
F 379
E 317
D 255
C 192
B 130
A 67.9

MAX. STRESS
441 MPa < ALLOW. = 494 MPa
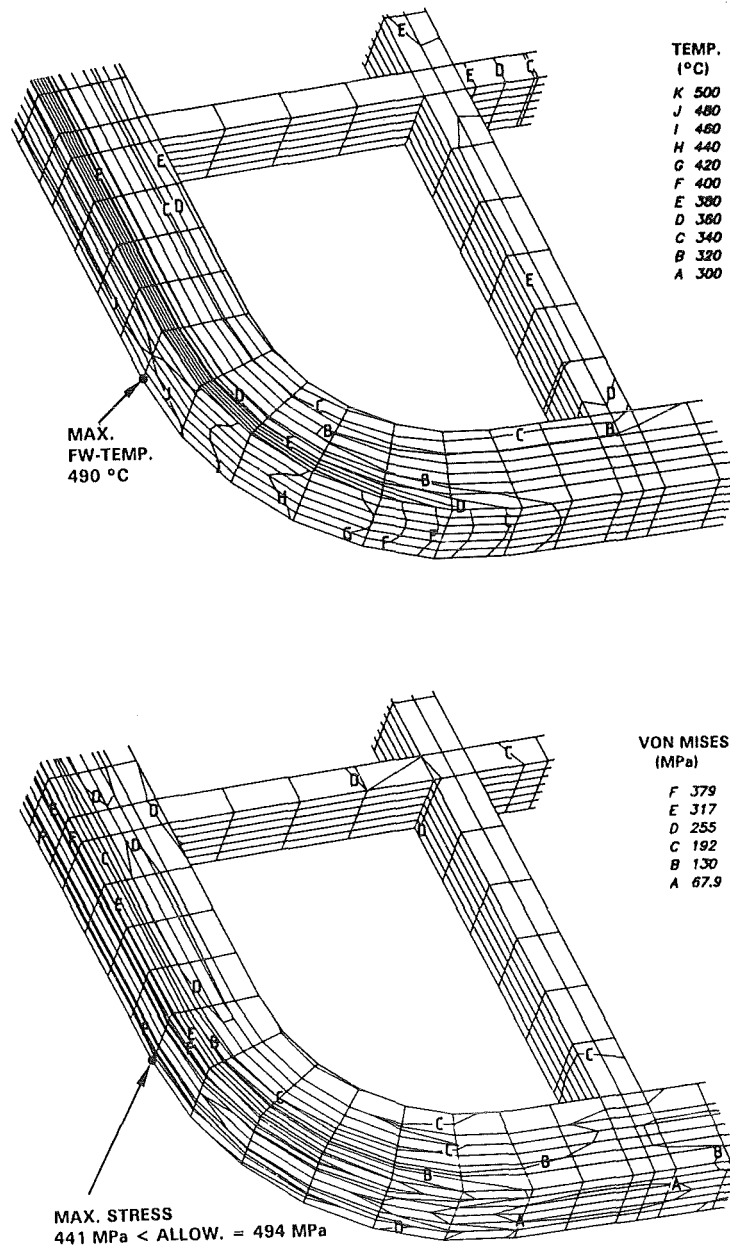
Fig. 2.6-2: Temperature (top) and stress distribution (bottom) in the blanket structure

441 MPa. This is well below the allowable total stress of 494 MPa according to ASME. This maximum stress can be reduced by further increasing the shield temperature.

The global thermomechanical behaviour has been investigated in an additional two-dimensional ABAQUS analysis for a radial/poloidal section of the outboard blanket segments [29]. These investigations show that the maximum thermal stress and the stress distribution in the first wall depend strongly on the support conditions of the segment and the temperature of the backward shield plate. The quasi plane strain conditions assumed in the three-dimensional calculation for the radial/toroidal section was confirmed to be reasonable in the case that bending of the segment is suppressed, e.g. by connecting the shield plates of the segments to a rigid toroidal shell. By op-

timizing the boundary conditions a reduction of the main compressive stresses of up to 28 % can be reached. The resulting von Mises stress must be determined in additional three-dimensional calculations.

The shield temperatures assumed in the two-dimensional calculations were in all cases lower than the mean value of the minimum and maximum temperature of the blanket structure. This allows the conclusion that also under operational transients the temperature difference between the shield and the structure, and consequently also the thermal stresses will not be larger than under the steady state conditons described above.

A preliminary assessment of the irradiation effects on the mechanical properties of MANET has been carried out following largely the recommendation given in [27]. The yield strength and ultimate tensile strengh increase with irradiation. It is therefore conservative to use the values for the unirradiated material. An important irradiation effect is the rise of the ductile to brittle transition temperature (DBTT). The coolant temperatures have been selected such that the minimum temperature of the structures is above the recommended maximum DBTT of 250 °C, a preliminary value which has to be confirmed. Irradiation induced swelling can be neglected for MANET below 100 dpa. Irradiation induced creep was estimated using a correlation derived from a broader experimental basis [30]. For the maximum total stress and a damage of 70 dpa, a creep value of only 0.02 % was calculated which is far below the admissible value. In summary it can be stated that irradiation effects in the structural material will neither lead to a significant loss of the load carrying capacity nor to untolerable deformations of the components.

3. Ancillary Loop Systems

For each of the two coolants - Pb-17Li and helium - a completely different system is required for heat and tritium extraction. All methods and components of the helium system are very similar to those designed for helium-cooled solid breeder blankets and are described for example in [31]. In the lead-lithium loops both the heat and the tritium are transported to the steam generators for extraction. Double-walled tubes are used in these heat exchangers where the liquid metal flows around the outer tube, the water in the inner tube and a secondary liquid metal (NaK) in the concentric gap between the tubes. Tritium diffuses through the outer tube wall into the NaK and is removed by batchwise cold trapping of this liquid metal. This ancillary loop system is described in [3].

The systems for helium and liquid metal cooling are completely independent but have to deliver their heat to the same steam cycle. A scoping study of this steam cycle resulted in the selection of a saturated steam turbine with about the same parameters as used in nuclear fission water reactors,

leading to an efficiency of 34 %. It would be possible to increase slightly the efficiency of the system by superheating the steam with the liquid metal but this would add complexity to the system. A layout of the proposed system is shown in Fig. 3-1. It can be seen that roughly half the feedwater flow is heated up to the boiling temperature by the low-temperature helium. Most of the evaporation heat is provided by the liquid metal.
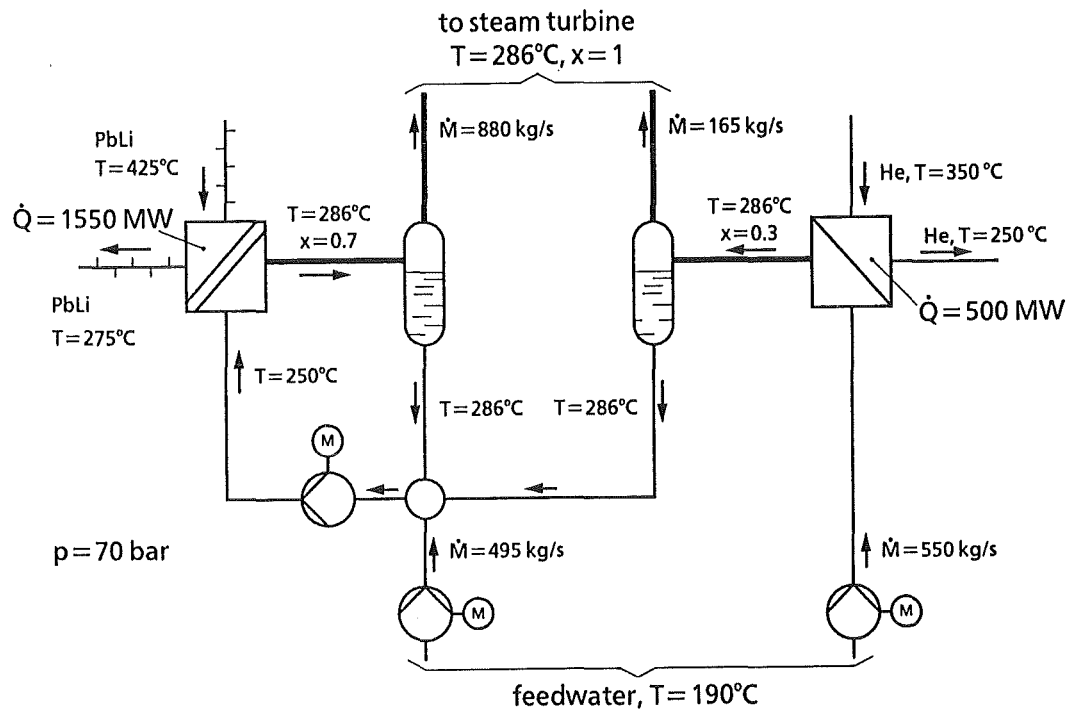
Fig. 3-1: Steam generating system for Dual Coolant Blanket

There are 80 liquid metal/water (steam) and 10 helium/water (steam) heat exchangers anticipated. This design provides a high redundancy (see Section 7) and leads to relatively small heat exchangers which can be easily replaced by spare components in case of malfunctions. An additional reason for the large number of liquid metal heat exchangers is the requirement of electrical insulation between inboard and outboard region and possibly between torus sectors. Recent studies of the transient electromagnetic effects performed in the frame of ITER have probably relaxed this requirement. In any case the number of helium loops can be kept smaller and is independent from the number of liquid metal loops.

4. Corrosion and Purification System in the Pb-17Li Loop

4.1 Compatibility of the Structural Material with Pb-17Li

The evaluation of long term corrosion tests of MANET steel in flowing liquid Pb-17Li eutectic alloy at 450 to 550 °C in the pumped PICOLO loop showed that the material did not suffer from internal corrosion effects. The material losses due to a material dissolution mechanism [32, 33] are the only noticeable corrosion effect. The results of the corrosion tests performed with a flow velocity of 0.3 m/s (turbulent flow) and measured near the test section inlet can be expressed by the equation

$$\log d_x = 12.3384 - 10960/T \text{ (with } d_x \text{ as the loss of wall thickness in } \mu\text{m/h}$$
$$\text{and T as the wall temperature in K).}$$

According to this equation, for example, an annual loss of 13.25 μm would have to be expected at a temperature of 723 K. The influence of typical parameters of the fusion reactor blanket, such as the strong magnetic field, the higher flow velocity, and the irradiation with high energy neutrons has to be considered. Since the magnetic field may suppress the turbulence of the flow of the liquid alloy, corrosion may be less than in the experimental facility. On the other hand, irradiation may enhance the diffusion rates in the solid material, faster diffusion may lead to higher corrosion rates. However, in the system MANET steel/liquid alloy corrosion is not characterised by solid state diffusion, it is mainly a process of the solid/liquid interface. It can, therefore, be expected that the irradiation does not significantly increase the liquid metal corrosion of MANET steel. The irradiation causes the formation of activation products, thus the liquid alloy dissolves certain amounts of activated material which may be precipitated in peripheral parts of the cooling system. The mechanical properties of MANET steel at temperatures up to 600 °C were not influenced by the presence of the eutectic Pb-17Li alloy [34].

Because of the compatibility of MANET steel with the liquid alloy, the functionality, feasibility and reliability of blanket components which are in contact with the flowing liquid alloy are not reduced. The necessity to coat the steel with an insulating surface layer for MHD reasons reduces further the corrosion problem in the self-cooled liquid metal blanket, since such a coating has a protective effect against liquid metal corrosion. The coating provides such a protection just at positions with the highest temperature and the fastest flow velocity, i.e. positions with most severe corrosion conditions.

4.2 Purification of Pb-17Li

Corrosion products as well as other impurities generated and/or activated by neutron irradiation are transported by the circulating breeder material and may be deposited in cooler parts of the

primary loop. This can cause a maintenance problem and is a safety concern in case of a liquid metal spill. A further problem is the risk of blocking narrow channels if the concentration of corrosion products becomes too high. For these reasons it is necessary to develop and employ suitable purification systems for continuous removal of impurities.

4.2.1 Removal of Corrosion Products

In the reference design the inner surface of all liquid metal ducts in the blanket segment are coated by an insulating layer. The coating material envisaged is alumina which has an excellent compatibility with Pb-17Li at the chosen interface temperature ($<$ 470 °C). The interface temperature outside the blanket segment where the breeder material is in contact with the structural material is at least 50 K lower. Therefore, the corrosion rate of alumina as well as steel will be low and the amount of corrosion products to be removed rather small. Different removal methods are under investigation including magnetic traps, cold traps, and isothermal traps characterized by a large surface for depositions achieved by arranging packs of wire mesh in the coldest part of the loop. These methods are presently tested in the TRITEX loop.

4.2.2 Removal of Radiotoxic Nuclides

The main impurities to be considered with regard to accidental spills of Pb-17Li are ^{210}Po and ^{203}Hg. ^{203}Hg is of importance since it contributes significantly to the radiological hazard. ^{210}Po is of special concern because it is an α-emitter. It is generated by neutron irradiation of bismuth which is both an original impurity of lead and a transmutation of lead caused by neutron capture. In the past, ^{210}Po was expected to yield the highest contribution to the ingestion dose. However, it has been shown [35] that the polonium volatility is much smaller than assumed before because it forms lead polonide in the eutectic, an intermetallic compound with a vapor pressure much lower than the one of polonium itself. Furthermore, neutronics calculations have shown, that the generation of ^{210}Po has been over-estimated in the past (see Sect. 2.4.4).

But nevertheless, it is desirable to limit the ^{210}Po content of the liquid metal breeder by either on-line removal of polonium or its precursor bismuth. Methods for the removal of both elements are under investigation. Experiments showed, that it may be possible to maintain a bismuth concentration below 10 ppm leading to a low enough ^{210}Po concentration without additional polonium removal.

4.2.3 Adjustment of the Lithium Concentration

For each tritium atom bred in the blanket one lithium atom is lost. An other potential "sink" for lithium is oxydation of the breeder material. Therefore it is necessary to add lithium enriched to

more than 90 % [6]Li in order to maintain a constant Li concentration and [6]Li content as well. It has been shown [36] that this adjustment is possible by adding higher melting Li-Pb compounds.

5. Tritium Control

The requirements on the blanket tritium removal and recovery system are a low tritium inventory in the total blanket system and an acceptable tritium loss through the steam generator into the water (assumed: 20 Ci/d for all reactor blankets). The latter requirement is the crucial one for a Pb-17Li blanket due to the low tritium solubility of Pb-17Li.

Two different methods to remove tritium from Pb-17Li have been investigated at KfK: Cold trapping in NaK and the use of solid getters in Pb-17Li. An assessment of the latter method [37] based on experimental results showed that it may become feasible if tritium permeation into the water can be reduced decisively (at least by a factor of 1000) by suitable coatings at the steam generator tubes. This is difficult to envisage and therefore the first method has been selected as reference solution. This method includes the following steps [3]:

a)   tritium permeation into the NaK-filled gap of the double-walled steam generator

b)   tritium removal from NaK by precipitation as tritide in a cold trap

c)   tritium recovery by thermal decomposition of the tritide at higher temperatures.

With respect to a) an assessment has shown that the permeation process influences sensibly neither the total tritium inventory nor the tritium losses. Therefore, no R&D work has been performed to prove the feasibility of this step. For b), tritium must be removed at very low concentration levels where the efficiency of cold trapping was questionable. With respect to c), again no relevant experimental results existed. Therefore, specific investigations on the kinetics of hydrogen removal and recovery were performed [38-41], tritium was simulated by [1]H.

The obtained results can be summarized as follows:

-      cold trapping efficiencies of $\eta > 75\%$ were obtained for blanket relevant conditions (temperatures, velocities, loading time period)

-      cold trapping can be well described with a diffusion limited model

-      about 99 % of the hydrogen is recovered in 3 hours at 400 °C.

These results confirm the concept of two removal/recovery cycles per day.

Based on the experimental results, a flow sheet (Fig. 5-1) is proposed for a tritium production rate of $\dot{m}_T$ = 5g/d for one blanket segment and a tritium loss from all blankets to the steam generator of 10 Ci/d (another loss of 10 Ci/d is assumed to occur in the helium cooling system). A permeation barrier on the water side is assumed which reduces permeation by a factor B = 100. Factors between 20 and 100 were reported for natural oxide layers at the water side without anticipating to increase artificially this value. Two cold traps are operated in parallel: one for cold trapping; the other for tritium recovery. For the latter purpose the cold trap is decoupled from the circulation loop, drained from NaK, heated up to temperatures of about 400 °C and the pumped off tritium gas is stored in a getter bed.

Using a protium addition of $\dot{m}_p/\dot{m}_T$ = 3 (method of isotope swamping) a cold trap efficiency of η = 0.75 can be acieved with inlet and outlet temperatures of T_{CTi} = 71 °C and T_{CTo} = 30 °C, respectively. Table 5-1 shows also values for higher permeation barrier factors (which are presently developed for other blanket concepts).

For a NaK velocity in the cold trap of $\approx$ 3 cm/s and a specific surface of 1000 m²/m³ (experimentally used values) a cold trap with a height of 1 m and a diameter of 0.8 m is required for the design value of B=100. For larger values of B, the diameter reduces, see Table 5-1. An assessment of the tritium inventory in the NaK (dissolved tritium) and in the cold traps
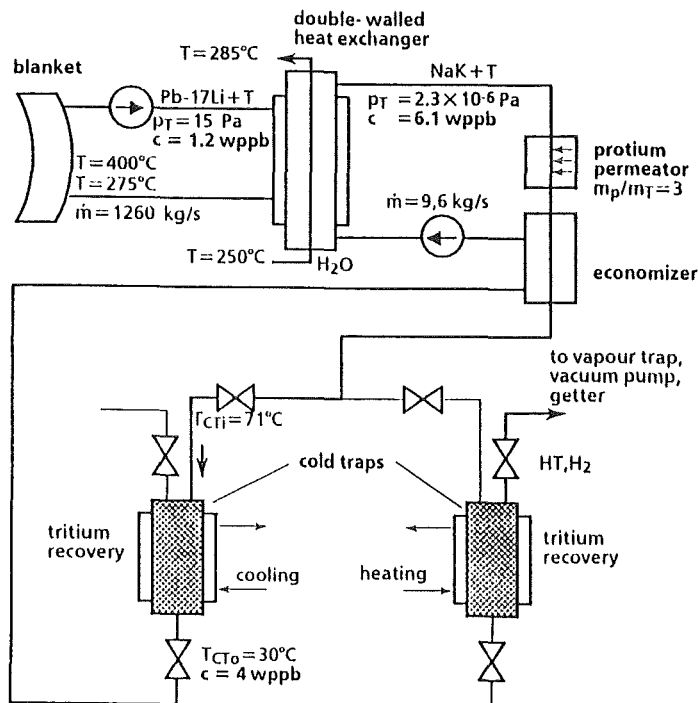
Fig. 5-1 Tritium flow sheet for a
DEMO blanket segment
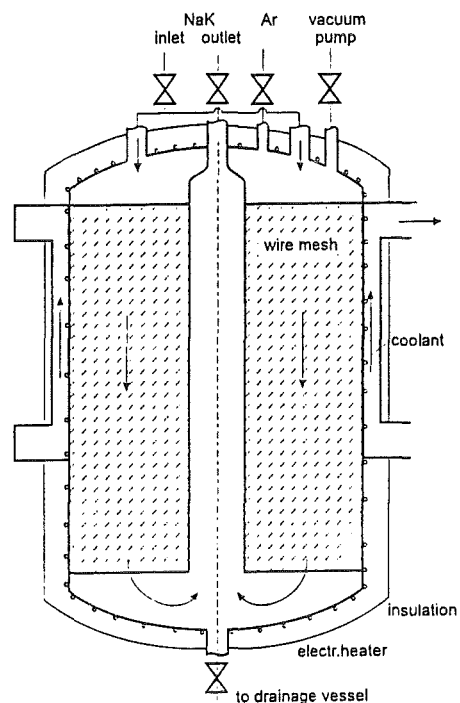
Fig. 5-2 Fusion blanket cold trap

Table 5.1 Tritium Removal/Recovery System for a DEMO Blanket Segment
($\dot{m}_T$ = 5g/d, η_{CT}=0.75, T_{CTo}=30 °C, V_{NaK} ≈ 3 cm/s)

permeation barrier factor B(1)	100	200	1000	2000
mass flow rate $\dot{m}_{NaK}$(kg/s)	9.6	4.4	0.8	0.5
Tritium concentrations (wppb)				
steam generator C_{SG}	6.1	12.1	60.1	121
cold trap inlet C_{CTi}	8.2	19.4	89.9	182
cold trap outlet C_{CTo}	4.0	4,8	31.5	60.5
isotopic swamping $\dot{m}_p/\dot{m}_T$ (kg/kg)	3	3	0	0
cold trap inlet temp. T_{CTi}(°C)	71	80	71	90
cold trap dimensions: height H (m)	1	1	1	1
diameter D (m)	0.8	0.6	0.3	0.2
tritium inventory: in NaK J_{NaK}(g)	0.01	0.02	0.06	0.11
in cold traps J_{Ct}(g)	2.5	2.5	2.5	2.5

(precipitated tritium) is also included. Values for the tritium inventories in the total blanket system are given in Table 6-1 (Sect. 6.1), valid for the design value of B = 100. For higher values of B, the tritium inventory in the steel and Pb-17Li increases only slightly.

Figure 5-2 shows schematically a cold trap with an annular wire mesh packing for precipitation which is countercurrently cooled by air and heated-up electrically (alternatively, NaK can be used as cooling/heating fluid). Drainage/refilling is carried out with an argon circuit and a dump tank.

An important feature of the proposed system is that no corrosion or radioactive products from the Pb-Li loop are transported into the tritium extraction system. No additional carrier fluid is required for tritium processing, therefore, only small volume flow rates have to be processed and a small number of process components is required. The separation of tritium from protium can be carried out in the hydrogen separation column of the fuel clean-up system.

The clean-up system in the helium coolant loop for tritium permeating from the plasma and Pb-17Li into the helium has not been considered in detail because tritium separation from helium is investigated in detail for helium cooled ceramic breeder blankets.

6. Safety and Environmental Impact

This section presents the scope of hazard potential and accidents related to the blanket system under the following topics: (1) toxic inventories, (2) energy sources for mobilization, (3) fault tolerance, (4) release of radionuclides, and (5) waste management. The assessment includes the intermediate NaK circuits for tritium recovery, but excludes auxiliary subsystems for storage, purification, drainage etc. which are not yet defined and will be subject to future analyses.

6.1 Toxic Inventories

Radioactive inventories in the different regions of the blanket (inboard, outboard, first wall, breeding zone and shield) as well as in the cooling systems have been assessed and are summarized in Table 6-1 in two categories, i.e., tritium and activation products. No chemical toxins, like beryllium, are included in the blanket design presented in this report.

Table 6-1 Radioactive inventories in blanket and related systems

Blanket region or system	Tritium (g)	Activation Products after shutdown (Bq)	
		0 s	1 year
Breeder material (Pb-17Li)	30	6×10^{20}	5.3×10^{16}
Primary first wall coolant (Helium)	0.15	1.5×10^{11}	0.5×10^{11}
Intermediate coolant (NaK)	1	negligible	negligible
Steam system	< 1.7	negligible	negligible
Tritium recovery system	200	negligible	negligible
Structural material (total)	19	1.5×10^{20}	5.2×10^{19}
First wall	7.2	5.2×10^{19}	1.9×10^{19}
Breeding zone	11.5	9×10^{19}	3.3×10^{19}
Shield	0.3	4.4×10^{18}	5.5×10^{17}
Insulating layers	negligible	2.1×10^{19}	4.5×10^{11}

The tritium inventory in the breeder (Pb-17Li) is determined by the recovery process (compare Section 5) and is moderate (30 g). A considerable amount of tritium ($\simeq 4$ g/d) will permeate into the helium coolant. This is assumed to be continuously removed via a by-pass flow. Applying the same rationale as used for quantifying the tritium inventory in the primary coolant of the solid breeder blanket (BOT) yields a tritium inventory of 0.15 g in 9000 kg of helium. The tritium inventory in

the intermediate NaK circuits depends on the achievable permeation barrier factor. For the reference case (B = 100) the tritium dissolved in the NaK of all blanket systems sums up to about 1 g. The tritium losses of 20 Ci/d (0.002 g/d), half of which coming from the NaK system and the other half from the helium cooling system, would accumulate to 1.7 g of tritium in the entire water/steam system, which is acceptable (compare Section 6.4). The tritium inventory in the recovery system is governed by the inventory in the cold traps and amounts to 2.5 g per circuit, i.e., 200 g for 80 circuits, corresponding to approximately one half of the daily production. The structural material will accumulate about 19 g of tritium with a weight concentration in the first wall of 72 wppb (compare Table 6-1).

Activation products inventories have been assessed as described in Section 2.4.4. The specific activity in the Pb-17Li after decay times of 0 s, 1 h, 1 d, 1 month, 1 yr amounts to 2.4×10^{14}, 1.1×10^{13}, 5.2×10^{12}, 1.4×10^{11}, 2.1×10^{10} Bq/kg, respectively. These numbers refer to the Pb-17Li in the first channel row (next to the FW) of the outboard blanket under the assumption that the liquid metal remained in place for the full irradiation time of 20000 hours. Accounting for a radial activation profile and for the actual residence time the circulating liquid metal spends in the flux region, a dilution factor of 10 has been assumed, leading to the values quoted in Table 6-1. Activation products in the first wall helium coolant are introduced by corrosion and sputtering. They have to be permanently removed, in order to avoid accumulation somewhere in the circuit components. Therefore, the contents are considered to be small, i.e., $< 1.5 \times 10^{11}$ Bq. The specific activity in the first wall (including impurities as specified in Section 2.4.4) after decay times of 0 s, 1 h, 1 d, 1 month, 1 yr is 5.7×10^{14}, 4.9×10^{14}, 3.5×10^{14}, 3.1×10^{14}, 2.1×10^{14} Bq/kg, respectively. It decays much slower than in Pb-17Li. In the breeding zone and shield the radioactivities are considerably smaller. The specific activity in the insulation layers has not been evaluated explicitly, but an estimation showed that it is negligible after a few minutes, except for very long times (see Tables 6-1 and 6-3).

6.2 Energy Sources for Mobilization

Potential energy sources in upset or accidental conditions are seen in (a) plasma disruptions, (b) continued plasma operation after cooling disturbances, (c) decay heat, (d) work potential of pressurized coolants, and (e) exothermic chemical reactions.

(a) Plasma disruptions can cause local evaporation of first wall material or mobilization of adhesive dust. This is a problem of first wall protection and dust processing that is common to all fusion reactors and not specific to a particular blanket system. The energy source is essentially the energy stored in the plasma, typically $\simeq$ 1 GJ. (b) Continued plasma operation after a sudden cooling disturbance will bring any first wall to melt within tens of seconds. The energy source is simply the time integral of fusion power from the cooling disturbance to complete shutdown. This time integral is inherently small (by plasma poisening) or otherwise a matter of plasma control

and of hypothetical scenario conventions, and again not peculiar to a specific blanket concept. (c) The decay heat is the governing feature in managing cooling disturbances like LOCA, LOFA (see Section 6.3) and, in particular, loss of site power or loss of heat sink. The decay heat in the entire blanket amounts to 53.2 MW after shutdown and declines after 1 h, 1 d, 1 month, and 1 yr to 10.8, 1.56, 1.22, 0.57 MW, respectively. (d) The first wall cooling system contains $\approx$ 9000 kg of helium at 8 MPa, $\simeq$ 300 °C. The work potential relative to ambient conditions is $\approx$ 13 GJ. Adiabatic expansion of the helium from two outboard first wall cooling circuits ($\approx$ 2100 kg), which are connected within a subsystem (see Section 7), would pressurize the vacuum vessel in the event of an in-vessel pipe rupture to $\approx$ 0.47 MPa absolute. This is above the expected design pressure ($\simeq$ 0.2 MPa) and, hence, would require an extra expansion volume. (e) Chemical reactions may occur between Pb-17Li and air or water in various accident scenarios. These processes have been reviewed in [42] and found to be moderate, since in Pb-17Li/water reactions only the lithium reacts and the kinetics is controlled by the small lithium mass fraction of only 0.7 %. For NaK/water reactions see Section 6.3.

6.3   Fault Tolerance

The following analyses of electromagnetic forces and temperature transients have been performed in order to show, whether this blanket system is tolerant against conceivable transients and accidental conditions.

Electromagnetic forces and induced stresses caused by disruptions have been analyzed with the CARIDDI code as it was done in [43]. The 3-D model covers one quarter of the blanket segment using poloidal and toroidal symmetry. The maximum von Mises stresses ranging up to 73 MPa are uncritical. The results are preliminary. Stress aggravating effects of less than a factor of two are expected from vertical plasma motion and from the fact that the material is ferromagnetic. Both effects need further code improvements. Stress relief by factors of 3 to 5 may be obtained by electrically bridging the segments at the first wall (compare [44]).

Temperature transients have been studied for instantaneous loss-of-coolant scenarios with leaks in one of the three primary coolant circuits per blanket segment (2 helium circuits for the first wall and one Pb-17Li circuit for the breeding zone), and in the intermediate NaK circuit. A LOCA in a first wall helium circuit means at most an instantaneous loss of helium at t = 0 in one of the two helium loops. Plasma shutdown is assumed to occur at t = 1 s with a linear decrease of the surface heat flux to zero in 20 s. A 3-D model representing two adjacent first wall cooling channels (one being intact and the other one failed) has been adopted in the FE analyses with FIDAP. Transient temperatures in the first wall exceed the steady state values for a few seconds by up to 100 °C before they decline and stabilize at a low level. The temperature transients do not endanger the integrity of the structure [45]. A LOCA in the Pb-17Li circuit can cause (a) a loss of liquid metal flow in the blanket in case of an ex-vessel leak, or (b) a drainage of the Pb-17Li from a blanket

segment in case of a major in-vessel leak. For (a) the decay heat in the structure plus Pb-17Li would lead to temperature rises, which would stabilize at $t_{Pb-17Li} < t_{He} + 50 \,°C$, if the first wall cooling remained intact (t_{He} = helium coolant temperature). For case (b) with all Pb-17Li removed but with the first wall cooling systems operating, an estimation revealed a maximum structure temperature $t_{structure} < t_{He} + 100 \,°C$. At $t_{He} = 350 \,°C$ this is slightly above the normal operating temperature. These transients do not endanger the integrity of the structure. A LOCA in the intermediate NaK circuit with the consequence of substituting the NaK in the steam generator tube gaps by the cover gas, e.g. argon, would reduce the heat transfer coefficient in the steam generator by 1 to 2 orders of magnitude, leading to a strong temperature increase of Pb-17Li at the steam generator outlet. In order to avoid excessive temperatures in the blanket, the plasma has to be shut down within approximately 60 s after drainage of the NaK. This scenario does not present a safety concern, but the temperature transients need further attention with regard to design limits of the structural material.

Pb-17Li/NaK or NaK/water leaks may be postulated for the double-wall steam generator. While the first type would lead to a limited LOCA in the Pb-17Li circuit, the second type would involve chemical NaK/water reactions which are exothermic and mostly violent. Such leaks have been assessed in [46] on the grounds of industrial experience in sodium technology with the result that a fast propagation of a single inner tube failure can be precluded [46]. Confirming tests are proposed.

6.4 Tritium and Activation Products Release

Radioactive effluents to the environment arise during normal operation and in the course of accidents. In normal operation they will be governed by tritium releases via the steam circuit for which a limit of 1 TBq/d serves as a guideline. The 20 Ci/d (0.74 TBq/d) of tritium specified in Section 6.1 as tolerable losses from the primary coolants to the water/steam system are below this limit.

The release rates in accidental situations are hard to quantify at this stage of analyses. For a first judgement on the radiological hazard potential an assessment has been made on the early dose equivalent (EDE) to the most exposed individual (at a distance of 1 km from the point of release) [47] caused by the inventory escaping into the vacuum vessel or containment in case of an accident. This inventory has been taken as the largest amount of fluid within the blanket system (Pb-17Li, helium or NaK) which could be liberated by a single failure (like a guillotine break) into the vacuum vessel or other compartments of the containment. A release factor of 1 has been postulated for this assessment, i.e., all the inventory escaping into the vacuum vessel or containment would at the same time be released to the environment. This is, of course, unrealistic. However, the EDE values thus obtained relative to allowable limits (e.g., 100 mSv recommended in [48] as a safety goal for ITER) give an idea of the tolerable release factor. This has to account for

physical-chemical processes governing the mobilization, as well as retention effects imposed by the different containment barriers. Table 6-2 summarizes the total radioactive inventory, the fractions escaping into the vacuum vessel or containment, and the fictitious EDE.

Table 6-2   Accidental tritium and activation products release into vacuum vessel and containment in case of LOCA

| | Total Inventory | Fraction escaping into | | Maximum inventory escaping into vacuum vessel or containment | Early dose equivalent (Release factor = 1) (Sv) |
		Vacuum vessel	Contain-ment		
Tritium	(g)			(g)	
Breeder material (Pb-17Li)	30	≈ 0.035	≈ 0.027	1.05	2×10^{-3}
Prim. FW coolant (helium)	0.15	0.24	0.24	0.036	6×10^{-5}
Intermediate coolant (NaK)	1	0	1/80	0.0125	2×10^{-5}
FW structural material	7.2	1	0	7.2	1×10^{-2}
Activation products	(Bq)			(Bq)	
Breeder material (Pb-17Li)	6×10^{20}	≈ 0.035	≈ 0.027	2.1×10^{19}	2×10^{3}
Prim. FW coolant (helium)	1.5×10^{11}	0.24	0.24	3.6×10^{10}	n.a.
Intermediate coolant (NaK)	n.a.	0	1/80	n.a.	n.a.
FW structural material	5.2×10^{19}	1	0	5.2×10^{19}	1×10^{5}

n.a. = not assessed

It can be seen from Table 6-2 that the tritium inventory in the breeder, primary coolant, intermediate NaK, and in the first wall structure would cause an EDE well below the 100 mSv limit even without any retention. On the other hand, the activation products in the breeder material (with ^{203}Hg contributing with >95 % and ^{210}Po with < 1 % when considering the reduced ^{210}Po content according to Section 2.2.4) call for a release factor of $<5 \times 10^{-5}$. In assessing this tolerable release factor it has to be taken into account that a) the release of Hg as well as Po is not governed by the vapor pressure of these elements but by the vapor pressures of the intermetallic compounds with lead (Po) and lithium (Hg) which are orders of magnitude lower, and b) the breeder material spilled remains liquid for a very limited time only since the afterheat in Pb-17Li decreases very fast. The radiological hazard from activation products in the helium coolant and NaK has not been assessed. Its radioactive inventory is small. The inventory in the

first wall structural material (10^5 kg) would yield the highest early dose equivalent if entirely released. However, the mobilization is extremely low for design basis accidents.

6.5 Waste Generation and Management

Only the decommissioning waste (no operational waste) is considered here. The masses, volumes, radioactivities, and afterheat are summarized in Table 6-3. The total amount of radioactivity in

Table 6-3 Radioactive waste of the blanket system
(after 20000 hrs of full power operation)

Blanket region or system	Total Mass (kg)	Total Volume (m^3)	Total radioactivity in Bq after			Decay heat (W/m^3)
			1 yr	100 yrs	10^5 yrs	1 yr
Breeder material (Pb-17Li)	25×10^6	2700	5.3×10^{16}	9×10^{13}	3.3×10^{13}	0.76
Structural material (total)	3.2×10^6	407	5.2×10^{19}	2.2×10^{15}	1.9×10^{13}	see below
First wall	10^5	13	1.9×10^{19}	5.7×10^{14}	5.1×10^{12}	2.4×10^4
Breeding zone	1.3×10^6	162	3.3×10^{19}	1.4×10^{15}	1.2×10^{13}	3.4×10^3
Insulating layers	3.6×10^3	1.3	4.5×10^{11}	4.5×10^{11}	4.0×10^{11}	1.1×10^{-3}
Shield	1.8×10^6	231	5.5×10^{17}	2.1×10^{14}	1.9×10^{12}	13

the blanket structure (MANET) sums up to 1.5×10^8 TBq at shutdown for all inboard and outboard segments according to Table 6-1. The contribution of each radionuclide has been calculated as described in Section 2.4 for different cooling times. The dominating nuclides in the activation parameters vary with time and activation parameter. For example, ^{55}Fe and ^{54}Mn dominate the specific activity at a cooling time of 1 year, and ^{91}Nb, ^{63}Ni, ^{93}Nb after 100 years. The contact γ-dose rate per kg of MANET in the first wall ranges up to 1.1×10^5 Sv/h, declining slowly. The IAEA low level waste (LLW) limit of 2×10^{-3} Sv/h is reached after about 10^5 years, and the hands-on limit of 2.5×10^{-5} Sv/h is met not sooner than 3×10^5 years. The total amount of radioactivity in Pb-17Li is 6×10^8 TBq at shutdown, decaying by $\simeq 7$ orders of magnitude within 100 years. The following nuclides dominate the specific acticity by more than 65 % at various times: ^{207}Pb (after 0 s), ^{203}Pb and ^{204}Pb (after 1 h), ^{203}Pb (after 1d), ^{203}Hg (after 1 month), ^{204}Tl (after 1 yr), ^{205}Pb and ^{108}Ag (after 100 years). The contact γ-dose rate of Pb-17Li reaches the LLW limit without any purification after 300 years, the hands-on limit after about 7000 years. In view of the high lithium enrichment needed (90 atom-% ^{6}Li) the liquid metal breeder is envisaged to be used for several

blanket life times or even for more than one reactor life time, since the burnt amount of lithium can be replaced as required (see Section 4.2.3).

7. Reliability and Availability

The reliability of the blanket segments and the pertaining cooling circuits determines the availability of the whole blanket system and hence, affects the availability of the whole plant. The blanket segments are of particular importance because here no redundancy is possible, i.e. all segments must be operable at the same time. In case of a defect, the blanket segment concerned must be exchanged. The time needed for this procedure - the mean time to repair (MTTR) - is another decisive factor for the blanket system availability.

The blanket availability has been evaluated by applying the method of fault tree analysis. The top event is the unavailability of the entire blanket system when it ought to be available. Basic events are mainly failures of welds, pipes, steam generators, and of active components like pumps, blowers and valves. The basic failure rates and the MTTR for the cooling systems outside the blanket segments are compiled in Table 7-1. The data which are derived from fission nuclear technology are applicable to the active components of the blanket system, the pipes and the steam generators [49,50]. However, with respect to the blanket segments - in particular the welds - adjustments of the failure rates [51] are necessary to account for the specific design and function of the related elements.

Tab. 7-1 Failure Modes and Failure Rates for the Breeder Blanket of the Dual Coolant Concept

Failure modes		Failure rate [1/h]	MTTR [h]	Ref.
Pipe failure outside vac.vessel	(He)	$3.0 \cdot 10^{-9}$	200	49
Pipe failure outside vac. vessel	(Pb-17Li)	$1.6 \cdot 10^{-9}$	200	49
SG failure 30 MW	(Pb-17Li)	$1.2 \cdot 10^{-5}$	1200	49
SG failure 35 MW	(Pb-17Li)	$1.4 \cdot 10^{-5}$	1200	49
SG failure 80 MW	(He)	$3.0 \cdot 10^{-5}$	1200	49
Valve failure	(He)	$3.0 \cdot 10^{-6}$	200	49
Valve failure	(Pb-17Li)	$5.0 \cdot 10^{-8}$	200	49
Pump mechanical failure	(Pb-17Li)	$5.6 \cdot 10^{-6}$	50	50
Pump control failure	(Pb-17Li)	$2.6 \cdot 10^{-5}$	10	50
Blower failure	(He)	$1.0 \cdot 10^{-4}$	200	49
EB weld	[m^{-1}]	$1.0 \cdot 10^{-9}$		51
Diffusion weld	[m^{-1}]	$1.0 \cdot 10^{-9}$		51
Longitudinal weld	[m^{-1}]	$1.0 \cdot 10^{-8}$		51
Butt weld	[m^{-1}]	$5.0 \cdot 10^{-9}$		51
Pipe bend (180°)		$1.0 \cdot 10^{-8}$		51
Pipe bend (90°) (assumed 0.5 of 180°)		$5.0 \cdot 10^{-9}$		
Straight pipe	[m^{-1}]	$7.0 \cdot 10^{-11}$		51

7.1 Blanket Segments

The reliability of the blanket segments is mainly determined by the failure rates and modes of the following types of welds: (a) the diffusion welds between the two FW plates with integrated cooling channels; (b) the EB double welds between the poloidal blanket segment sections, and (c) the logitudinal welds connecting the FW and the inner plates forming the Pb-17Li ducts. Furthermore, the pipes between the blanket box and the top flange have to be taken into account. All other failures are not expected to influence significantly the segment unavailability and have been ignored.

The basic failure rate of diffusion welds is typically 10^{-9} (mh)$^{-1}$. Application of this number to all diffusion welds (typ a) of the blanket would be rather conservative because leaks of these welds can be tolerated as long as they do not endanger the structural integrity. Exceptions are those welds which are immediate neighbours to the EB double welds. Hence, a more realistic approach is to apply the failure rate of 10^{-9} (mh)$^{-1}$ only to the diffusion welds located next to the EB welds, and to ignore the others.

The failure rate of EB welds (type b) of 10^{-9} (mh)$^{-1}$ given in Table 7-1 is by a factor of ten less than that of a conventional nuclear weld [51]. In spite of the high thermal and mechanical load of the FW, the use of this number is reasonable because in the present blanket concept the EB weld comprises actually two independent welds with an intermediate leak detection gap, and both welds must fail at the same time to cause the unavailability of the blanket segment. However, to be conservative also a value of 10^{-8} (mh)$^{-1}$ has been used in the reliability calculations.

Leaks of the longitudinal welds (type c) inside the box can be tolerated as long as they do not impair the structural integrity of the blanket segment. Therefore, it is justified to use in the calculations a failure rate of 10^{-9} (mh)$^{-1}$ which is by a factor ten less than the value given in Table 7-1.

The MTTR needed to exchange a blanket segment has been varied in the calculations between 720 and 2160 hours (one and three months) to account for the uncertainties which still exist on this operation.

The results of the analysis are compiled in Fig. 7.1-1 which shows the availability of the totality of the blanket segments as a function of the MTTR. The three cases are defined as follows:

Case 3:   Specific failure rate of the EB weld increased by a factor of 10 to
           10^{-8} (mh)$^{-1}$; all diffusion welds taken into account

Case 2:   As Case 3, but only diffusion welds neighbouring EB welds considered.

Case 1:   As Case 2, but failure rate of EB welds 10^{-9} (mh)$^{-1}$ according to Table 7-1

Depending on the parameters used, the blanket availability varies between 0.73 and 0.97. The contribution of the different failure modes to the unavailability depends on the case. E.g. in Case 1, 10 % of the unavailabilities are caused by failures of the diffusion welds, 6 % by the EB welds, 37 % by the longitudinal welds, and the remainder by the tube systems outside the blanket box. About 2/3 of the overall unavailability is caused by outboard segment failures, 1/3 by inboard segment failures.
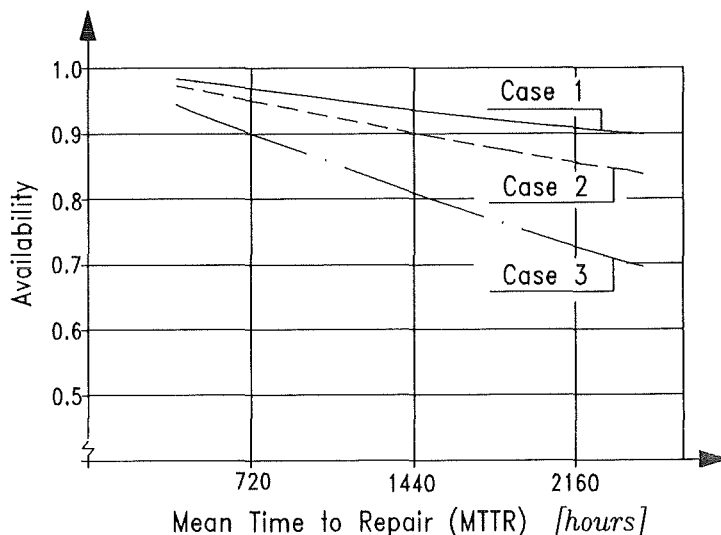

Fig. 7.1-1   Availability of the Dual Coolant Blanket

7.2   Cooling Systems

Separate cooling systems are provided for the inboard and outboard blanket for both helium and Pb-17Li (Fig. 7.2-1). The inboard as well as the outboard helium systems are subdivided into two independent subsystems. Each blanket segment is connected to both subsystems (see also Sect. 2.2). The helium subsystems for the inboard FW cooling consist of two, and for the outboard first wall of three circuits. The thermal power of the 10 circuits is 80 MW each. The circuits of the inboard subsystems are arranged in a two out of two redundancy, the circuits of an outboard subsystem in a two out of three redundancy (two out of two means, that the cooling will fail only if both systems fail). The liquid metal cooling systems of the inboard as well as of the outboard blanket are subdivided into 16 subsystems. The subsystems for the inboard blanket consist of 2 circuits with 30 MW each and for the outboard blanket of 3 circuits with 35 MW each. Each inboard subsystem builds a redundancy group two out of two, and each outboard subsystem a redundancy group two out of three. In each redundancy group, He as well as liquid metal, the failure of one circuit is tolerable.

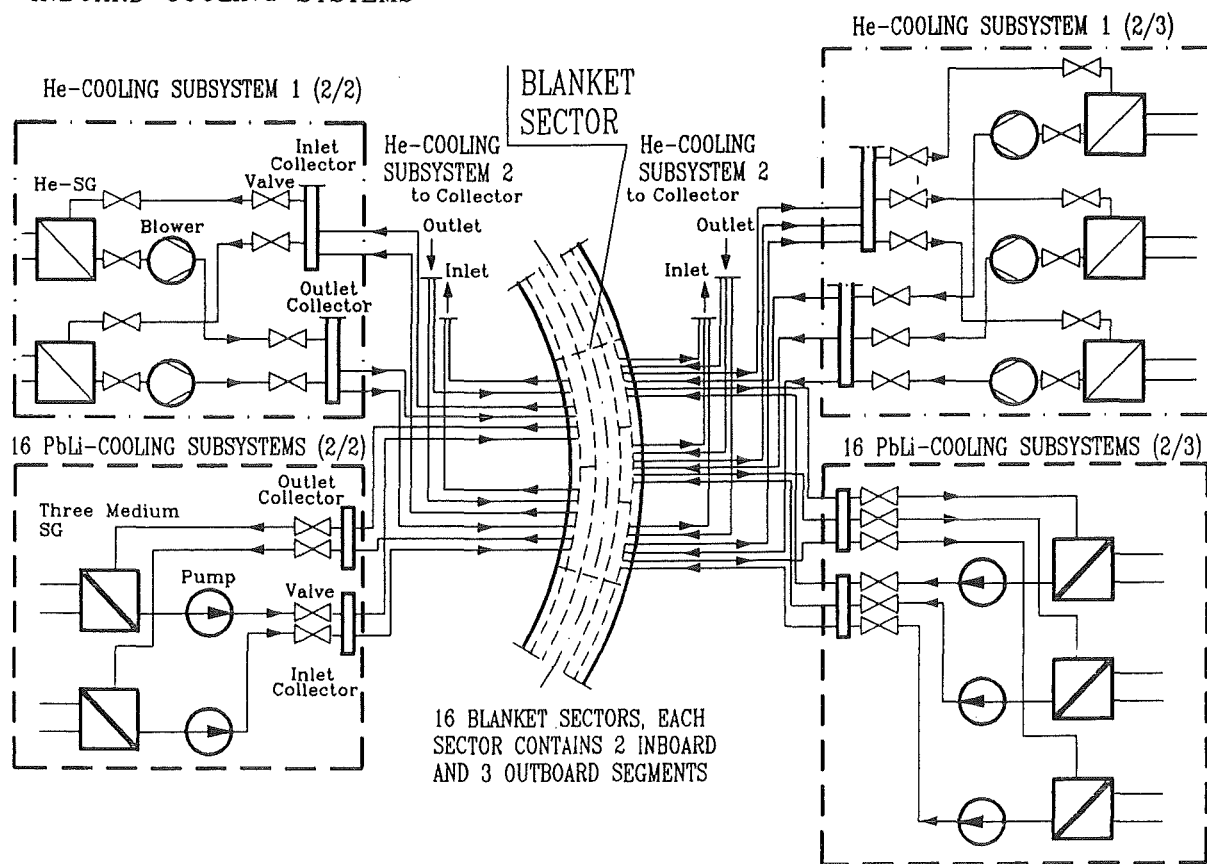INBOARD COOLING SYSTEMS   OUTBOARD COOLING SYSTEMS

Fig. 7.2-1   Helium- and liquid metal cooling systems

The availability for the cooling system is determined >97 % [52], depending on the MTTR in Tab. 7-1. The relative individual contributions to the unavailability are: 14 % by the inboard liquid metal system, 8 % by the inboard He system, 54 % by the outboard liquid metal system, and 23 % by the outboard He system. Regarding the liquid metal systems, the main contribution is due to the steam generators, in the He systems it is due to the steam generators and the blowers. Improvements of the availability appears to be possible by increasing the degree of redundancy, without changing the component design itself. In the liquid metal system the degree of redundancy will also be influenced by the possibility of solving the insulating problem between the circuits. In terms of design there is still a potential of increasing the availability, e.g. by increasing the number of valves, which has been demonstrated by the analysis of an earlier liquid metal blanket [50].

7.3   Conclusions

Because of the incompleteness of the design and the insufficient data base, the results obtained must be considered as preliminary. This is in particular true for the blanket segments. Nevertheless, the results are being considered as sufficient at the present stage of the project and confirm

the expectation that the required high reliabiliy is in principle achievable. Case 3 with the lowest availabities is based on very conservative assumptions; this case can be considered as a pessimistic lower boundary. The assumptions made in Case 1 are judged as realistic, but have partially to be confirmed in future work. With this respect, an experimental programme is carried out by KfK in collaboration with industry to develop and qualify the required welding and inspection techniques. The experiments are accompagnied by theoretical investigations of the temperature and stress distribution during welding [8].

The reliability of the cooling circuits is rather high; hence, these systems do not affect the overall blanket system availability significantly. If needed, a further increase in the reliability could be achieved by increasing the degree of redundancy.

8. Electrical Insulators

8.1 Development of Alumina Coatings on MANET steel

As outlined in Sect. 2.5, electrically isolating coating of the inner surfaces of the liquid metal ducts in the blanket segments is envisaged to reduce the MHD pressure drop. Alumina (Al_2O_3) which is an electrically insulating ceramic material of very high resistance has been proved to be compatible with the eutectic Pb-17Li alloy [53]. Therefore, the fabrication of alumina layers on MANET steel is being developed. The process involves the formation of an Al-rich intermediate layer on which alumina is formed by means of gaseous oxidation. The intermediate iron-aluminide layer is formed in a "hot-dip process" by dipping sheets of the steel into molten aluminum at a temperature of 800 °C. The steel covered with the intermetallic surface layer is then heated in flowing oxidizing gas (air or Ar/5 % H_2 saturated with H_2O at room temperature) to 950 °C. An oxide layer of 5 µm thickness is formed in about 30 hours [53]. The resistivity of such a layer is in the order of 10^{11} Ωm (at room temperature), if the layers are without defects. The alumina layers on iron aluminide coated MANET steel are stable against corrosion by liquid Pb-17Li alloy at 450 °C for 10000 hours [54]. The resistivity of the oxide layer was not reduced due to the exposure to the liquid alloy and the subsequent cleaning process. The interaction of the iron-aluminide sublayers with the steel matrix at this temperature was negligible. Neither was there any effect on the layer due to ingression of iron, nor was the steel affected by diffusion of Al into the martensitic structure, as could be shown by means of measurements of the hardness [55].

Self-healing of alumina layers after the formation of local defects has to be proved. Thermodynamic considerations indicate that it can be achieved by providing oxygen to the system in an adequate way in order to oxidize aluminum which is present below the alumina layer in form

of an intermetallic compound or solid solution in which the chemical activity of Al may be far below unity.

Another effect of the coating is the suppression of the liquid metal corrosion of MANET steel, since the alumina layers proved to be protective against corrosion. It is not yet known, if the insulating layers might also prevent the wetting of the materials. Several ceramic oxides as stabilized zirconia are wetted by Pb-17Li at > 350 °C. With incomplete wetting the insulating character of alumina layers may be conserved for some time after the occurence of small cracks.

Although the adherence of the intermediate layer on the steel and of the insulator on the intermediate are excellent, their behaviour in contact with the Pb-17Li alloy under thermal cycling conditions will be studied in 1994/95 using a loop of ENEA at Brasimone.

Some work has still to be done to optimize the fabrication conditions of the alumina layers. An apparatus for aluminizing larger components and tubes is in preparation. The "hot-dip process" will be modified in the way, that aluminizing may be performed by means of pumping aluminum at 800 °C through prepared components. These intermediate layers have to be oxidized in-situ. Quality control methods for the application inside of blanket segments have to be developed.

8.2 Irradiation Behavior of Alumina

During plasma operation, the insulator placed between the circulating liquid metal coolant and the surrounding steel structure to limit the MHD pressure drop is subjected to a neutron flux of about 1×10^{15} n/ (s cm^2), an applied electrical field of 1 kV (DC)/cm and a temperature up to 450 °C. The full power blanket life-time of 20 000 h results in a neutron damage in Al_2O_3 of 45 dpa.

Irradiation behavior of ceramics with a simultaneous application of electric fields has been investigated only in the recent years. In the course of these investigations, E. Hodgson discovered the so-called "radiation induced electrical degradation" (RIED) effect [56]. As a result of this effect, high-energy radioactive irradiation of ceramics causes in addition to the already known radiation induced electrical conductivity (RIC) also a considerable permanent increase in conductivity at a certain radiation dose when an electric field is applied. According to the present knowledge, the RIED effect is caused by colloid formation.

Irradiation experiments on Al_2O_3 have been carried out at several places of the world using electrons, protons, alpha radiation and neutrons. It was found out that not only the type of radiation, but also the temperature, voltage, dpa rate, dpa dose as well as the ratio of ionization rate to dpa rate represent important parameters influencing the behavior of the RIED effect. Furthermore, the content of impurities in the ceramics may be of influence which was observed in recent irradiation tests [57] performed in the KfK Dual Beam Test Facility in high vacuum at 450°C with an electrical field of 1 kV/cm using a 104 MeV α-particle beam. There was a great difference in the ir-

radiation behaviour between highly pure Vitox-alumina (99.9 %) and the less pure Wesgo-alumina (99.2 %) as can be seen in Fig. 8.2-1. The Vitox specimen (dimensions 7 x 10 x 0.3 mm) showed nearly no difference between the in-beam and out-of-beam conductivity but the highest RIED effect, and reached at 0.015 dpa a saturation level of the conductivity near 4 x 10^{-2} $(\Omega m)^{-1}$. For the lower-purity Wesgo specimen the in-beam conductivity was roughly two orders of magni-
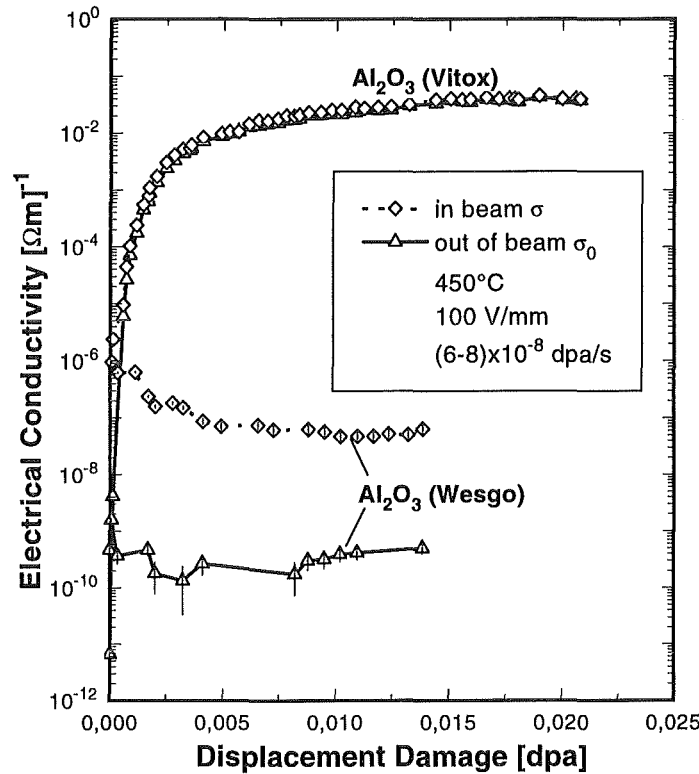
Fig. 8.2-1   Electrical conductivity as function of displacement damage for two
different alumina qualities

tude higher than the out-of-beam value (RIC effect) but a slight decrease of the conductivity during the irradiation time has been observed, reaching a saturation level of 10^{-7} $(\Omega m)^{-1}$ at 0.005 dpa. This value is four orders of magnitude lower than the highest tolerable value which has been estimated as 10^{-3} $(\Omega m)^{-1}$ for a 10 μm thick layer [58].

The saturation effect has been observed in almost all irradiation experiments carried out so far. However, in these tests the damage was below 0.5 dpa [59]. It is therefore necessary to carry out experiments with higher damage. This will be done by irradiating 0.5 mm thick Al_2O_3-plates with high-energy neutrons ($E_n \geq 0.1$ MeV) at a temperature of 450 °C and electrical fields of 1 kV(DC)/cm in the HFR (Petten) [59]. The irradiation will start early in 1995. At the end of 1995 a damage of about 7 dpa will be reached. Insulating coatings as fabricated by the processes described in Sect. 8.1 will be investigated both in the Dual Beam Test Facility and in the HFR (Petten).

9. Remaining Critical Issues, Required R & D Programme

Most of the critical issues of the four candidate blanket concepts being developed within the EU Fusion Technology Programme during the last five years have been investigated to a point that an assessment of the four concepts is possible leading to a selection of the two most promising ones at the end of this year. The remaining open questions are mostly related to the behaviour under irradiation which requires an ongoing experimental programme.

Two of the four concepts use the liquid metal Pb-17Li as breeder material. One common issue for both concepts is the activation of Pb-17Li under neutron irradiation [60]. The α-emitter ^{210}Po is especially a concern in case of a liquid metal spill. This nuclide is formed by neutron irradiation of bismuth, which can be present as impurity in the original Pb-composition and/or build up by neutron irradiation of lead. Recent experiments [35] have shown that the release rate of polonium is determined by the vapor pressure of an intermetallic Po-Pb compound which is orders of magnitude lower than that of polonium. Therefore, the release of ^{210}Po is by far not as critical as was expected a few years ago. Nevertheless, it is desirable to develop on-line Bi removal techniques in order to limit the Bi level to <10 ppm resulting in less than 0.2 ppb of ^{210}Po in self-cooled blankets without needing to remove polonium itself.

A second common issue of both liquid metal breeder blankets is the coating of the structural materials which serves either as a tritium permeation barrier in water-cooled blankets or as an electrical insulator in self-cooled concepts. For both purposes an alumina layer with an aluminum-rich sublayer is envisaged. The fabrication technology of such duplex layers, their compatibility with Pb-17Li and especially their long-term performance under irradiation have to be investigated further.

The main feasibility issue of the dual coolant concept is the electrical insulation between the flowing liquid metal and the load-carrying duct walls. The most attractive solution are insulating coatings on the duct surface. The Radiation Induced Electrical Degradation (RIED) of such layers has to be quantified by suitable irradiation tests, using ion-accelerator sources as well as fission reactors. Another crucial issue of coatings is the influence of imperfections (cracks, spallations) on the liquid metal flow. Estimates showed that such imperfections are tolerable only if there is a sufficient self-healing mechanism [58]. The aluminum-rich sublayer below the ceramic coating, if exposed to the liquid metal, reacts with the oxygen dissolved in it. This would lead to the growth of a new layer of alumina. This mechanism and its kinetics at the operating temperature have to be proven experimentally.

The required blanket R & D programme can be divided into the following groups:

1) Work necessary for all selected blanket concepts.

2) Investigation of issues which either determine the feasibility of a concept or have a decisive influence on its attractiveness.

3) Detailed analysis and tests to optimize a concept and to demonstrate its performance.

4) Development and testing of ancillary loop components.

The programme should mainly be concentrated in the next years on groups 1) and 2).

9.1 Work Necessary for All Selected Blanket Concepts

During the last three years the design of the segment box including the FW cooling channels became very similar for all four concepts. It should be possible to select and develop a manifolding system and fabrication technologies for the segment box which can be applied to each of the four concepts. A large emphasis has to be placed on the reliability of this box which is a crucial issue of all blanket concepts.

Further studies are necessary on the handling of in-vessel components, the methods and tools necessary for remote connection and separation of pipes, and on the time periods needed for the exchange of blanket segments which influences significantly the availability of the system.

9.2 Specific Issues of the Dual Coolant Blanket Concept

9.2.1 Insulating Coatings

The main feasibility issue of this concept is the electrical insulation between the duct walls and the flowing liquid metal. Insulating coatings on the duct wall surface in direct contact with the liquid metal are the most attractive solution. Such coatings need further development and testing especially under irradiation. The programme concentrates on the following issues:

a) Fabrication of a duplex layer with an aluminum-rich sublayer between the insulator ceramics and the structural material.

b) Investigation of a self-healing mechanism if the ceramic layer in contact with the liquid breeder cracks or flakes.

c) Radiation Induced Electrical Degradation (RIED) of the insulator under the combined loading of damaging irradiation, ionizing irradiation and electrical field.

9.2.2 Purification of the Liquid Metal Breeder

A low concentration of radioactive impurities such as corrosion products and especially the α-emitter ^{210}Po is important for safety and maintenance reasons. The development of suitable purification methods should be therefore continued.

9.2.3 Magneto-hydrodynamics Issues

MHD pressure drop is no longer an issue if insulating coatings are feasible. The prediction of three-dimensionally flowing electrical currents which have a great influence on velocity profiles and flow distribution in insulated ducts, however, requires additional theoretical and experimental work. Another subject of the ongoing MHD work is the investigation of a special kind of turbulence in strong magnetic fields which can enhance heat transfer and may allow an even more simple blanket design.

9.3   Concept Optimization and Performance Demonstration

Additional design work is necessary to study the arrangement of the connecting pipes in the region of the blanket port, the detachable connections between the blanket box and the shield, and the cooling of the shield.

Further analyses should be carried out to optimize the concept with regard to the thermal and mechanical loads of the structures. Important items are the dimensions of the FW cooling channels, the temperature of the shield, and the support conditions. The temperature and stress calculations must be completed by analysing singularities like the junction area between the box sections, the bottom plate and the upper tube plate.

Finally, more detailed analyses should be carried out on time dependent effects like operational transients and deformations due to thermal/irradiation induced creep and ratcheting.

10. Conclusions

The design of the Dual Coolant Blanket concept and the accompanying R & D work have reached a status where the feasibility, the attractiveness compared to other blanket concepts, and the required additional R & D work can be judged. The overall conclusions are:

- The concept has a potential for high safety and reliability due to a leak-tolerant design, a real double containment of the liquid metal breeder, redundant and diverse cooling systems (helium, liquid metal), large margins for internal pressure and additional loads, e.g. caused by plasma disruptions. A LOCA with delayed plasma shutdown results in a temperature increase of less than 100 K for a few seconds only. Each one of the three independent cooling systems is sufficient for afterheat removal below normal operating temperatures.

- The radiological hazard from accidental release of Pb-17Li is mainly determined by ^{203}Hg. The release of ^{210}Po is no longer a feasibility issue since both the generation and the release rate of this isotope are orders of magnitude lower compared to previous investigations.

- The design meets the boundary conditions (geometry, power density, performance, lifetime) of the DEMO reactor specified as a basis for blanket selection.

- The manufacturing of the blanket segment with dismountable shielding zone, integrated helium manifolds and leak detection system is relatively simple, and possible with available or near future technology.

- The analyses performed show that all temperatures and pressure drops are well within acceptable engineering limits.

- MHD pressure drop is no longer an important issue if the feasibility of insulating coatings can be proven. The pressure drop would be higher but still manageable if flow channel inserts have to be used.

- The maximum liquid metal temperature in the blanket is limited by strength consideration rather than by the corrosion in Pb-17 Li. This is especially true if alumina coatings are used in the blanket segment which have an excellent compatibility with Pb-17 Li.

- The feasibility of the proposed tritium extraction method from Pb-17Li, based on diffusion through the steam generator tubes into a secondary liquid metal (NaK) where it is removed from by cold trapping, has been proven experimentally. Sufficiently low tritium permeation losses can be achieved and the regeneration time of the cold traps allows for a cycling time of less than one day for the batchwise tritium recovery.

- Tritium extraction from the helium used for FW cooling is investigated in the frame of the solid breeder blanket development.

- Cooling of the FW by helium increases the complexity of the cooling system compared to an ideally self-cooled blanket concept. However, more than one external system is required for all liquid metal breeder blankets in order to extract tritium from the blanket segments, to ensure reliable afterheat removal, and to prevent freezing of the breeder material in case of an external malfunction.

- Self-cooling of the liquid metal breeder zone is the key element of an attractive blanket concept for a power reactor provided the feasibility of electrical insulation between liquid metal and blanket structure can be proven. The investigations of the Radiation Induced Electrical Degradation (RIED) of insulating coatings as well as the mandatory self-healing of a ceramic layer in contact with the liquid metal breeder requires an ongoing R & D programme over the next three years.

11. References

[1]   E. Proust, L. Anzidei, G. Casini, M. Dalle Donne, L. Giancarli, S. Malang, Breeding blanket for DEMO, Fusion Engrg. & Des. 22 (1993) 19-33.

[2]   L. Giancarli, L. Baraer, B. Bielak, M. Eid, M. Fütterer, C. Nardi, E. Proust, L. Petrizzi, J. Quintric-Bossy, J.F. Salavy, Y. Severi, European reference design of the water-cooled lithium-lead blanket for a demonstration reactor, Proc. of the 11th TMTFE, New Orleans, Lousiana, USA, June 19-23, 1994.

[3]   S. Malang, J. Reimann, H. Sebening (ed.), DEMO-relevant test blanket for NET/ITER, Part 1: Self-cooled Liquid Metal Breeder Blanket, Vol. 1 and 2, KfK 4907 and 4908 (1991)

[4]   S. Malang, E. Bojarski, L. Bühler, H. Deckers, U. Fischer, P. Norajitra, H. Reiser, Dual-coolant liquid metal breeder blanket, 17th SOFT Rome, Italy, Fusion Technology 1992, 1424-1428.

[5]   C.B. Reed, T.Q. Hua, D.B. Black, I.R. Kirillov, S.I. Sidorenkov, A.M. Shapiro, I.A. Evtushenko, Liquid metal MHD and heat transfer in a tokamak blanket-slotted coolant channel, IEEE/NPSS Fusion, 15th Symp. on Fusion Engineering, Hyannis, MA, Oct. 12-15, 1993.

[6]   K.J. Mack, R. Kirchner, M. Frank, R. Stieglitz, MHD heat transfer and pressure drop in electrically insulated channels at fusion relevant parameters, 18th SOFT, Karlsruhe (1994)

[7]   Siemens AG, internal report (1993)

[8]   L. Cizelj, H. Riesch-Oppermann, An Analysis of Electron Beam Welds in a Dual Coolant Liquid Metal Breeder Blanket, KfK 5360 (1994)

[9]   J. F. Briesmeister (Ed.): MCNP - A General Monte Carlo Code for Neutron and Photon Transport, Version 3A, Report LA-7396-M, Rev. 2, Sept. 1986

[10]   P. Vontobel, A NJOY Generated Neutron Data Library Based on EFF-1 for the Continuous Energy Monte Carlo Code MCNP, PSI-Bericht Nr. 107, September 1991

[11]   U. Fischer, Die neutronenphysikalische Behandlung eines (d,t)-Fusionsreaktors nach dem Tokamakprinzip (NET), KfK 4790 (1990)

[12]   U. Fischer, Impact of Ports on the Breeding Performance of Liquid Metal and Solid Breeder Blankets in the DEMONET Configuration, Fusion Engineering and Design 18 (1991), 323-329

[13]   H. Tsige-Tamirat, U. Fischer, Three-dimensional Activation and Afterheat Analysis for the Dual Coolant Liquid Metal Breeder Blanket, KfK 5402 (to appear)

[14]   R. A Forrest, D. A. J. Endacott, FISPACT - User Manual, AERE-M 3654(Rev), July 1990

[15]   J. Kopecky, H. A. J. van der Kamp, H. Gruppelaar, D. Nierop, The European Activation File EAF-2 with Neutron Activation and Transmutation Cross Sections, ECN-C-91-073, July 1991

[16] J.-Ch. Sublet, Elemental composition of structural materials including impurities and tramp elements, SEAFP/R-A6/2(93), October 1993

[17] M. Schirra et al., Untersuchungen zum Vergütungsverhalten, Umwandlungsverhalten und der mechanischen Eigenschaften am martensitischen Stahl 1.4914 (NET-Charge MANET-1), KfK 4561 (1989)

[18] U. Fischer, E. Wiegner, Production of ^{210}Po in Pb-17Li: Assessment of Methodological and Data Related Uncertainties, 17th SOFT, Rome, Italy, Fus. Techn. 1992, Vol. 2, 1719-1723

[19] L. Barleon, V. Casal, L. Lenhart, MHD flow in liquid-metal-cooled blankets, Fus. Eng. and Design 14, (1991), 401-412

[20] L. Barleon et al., Investigations of liquid metal flow through a right angle bend under fusion relevant conditions, 17th SOFT Rome, Italy, Fus. Techn. 1992, Vol. 2, 1276-1280

[21] L. Bühler, Liquid metal flow in arbitrary thin-walled channels under a strong transverse variable magnetic field, Fus. Eng. and Design (1991), 215-220

[22] L. Bühler, Additional magnetohydrodynamic pressure drop at junctions of flow channel inserts, 17th SOFT Rome, Italy, Fus. Techn. 1992, Vol. 2, 1301-1305

[23] L. Bühler, S. Molokov, Magnetohydrodynamic Flows in Ducts with Insulating Coatings, KfK 5103 (1993)

[24] S. Molokov, Liquid metal flows in manifolds and expansions of insulting rectangular ducts in the plane perpendicular to a strong magnetic field, KfK 5272 (1993)

[25] J. Reimann et al., First Results from Different Investigations on MHD Flow in Multichannel U-Bends, 7th Intern.Beer Sheva Seminar on MHD Flows and Turbulence, Jerusalem, Israel, February 14-18, 1993.

[26] P. Norajitra, KfK internal report (Jan. 93)

[27] Material Data Base for the NET Test Blanket Design Studies, compiled by M. Küchle, KfK (Febr. 90)

[28] E. Zolti et al., Interim Structural Design Criteria for Predesign of the NET Plasma Facing Components (1. Edition), NET/IN/86-14 (1986)

[29] H. Gerhardt, KfK internal report (1994)

[30] K. Herschbach, KfK personal communication

[31] M. Dalle Donne (ed.), DEMO-relevant Test Blankets for NET/ITER, Part 2: BOT Helium Cooled Solid Breeder Blanket, Vol. 1 and 2, KfK 4928 and 4929 (1991)

[32] H.U. Borgstedt, and D. Röhrig, Recent Results on corrosion behaviour of MANET structural steel in flowing Pb-17Li eutectic, J. Nucl. Mater. 179-181 (1991) 596-598.

[33] H.U. Borgstedt, G. Frees, and Z. Peric, Material compatibility tests with flowing Pb-17Li eutectic, Fusion Engng. and Design 17 (1991) 179-183

[34] H.U. Borgstedt, G. Frees, M. Grundmann, and Z. Peric, Corrosion and mechanical properties of the martensitic steel X18CrMoVNb 12 1 in flowing Pb-17Li, Fusion Engng. and Design 14 (1991) 329-334

[35] H. Feuerstein et al., Behavior of Po-210 in molten Pb-17Li, 5th Int. Conf. on Fusion Reactor Materials, Clearwater/USA (1991), Journal of Nucl. Mat. 191-194 (1992), 288

[36] H. Feuerstein et al., Eutectic mixture Pb-17Li in-situ production and Li-adjustment, 18th SOFT Karlsruhe (1994)

[37] J. Reimann, H. Feuerstein, Cold trapping for tritium from a self-cooled Pb-17Li blanket, 16th SOFT, Fusion Technology 1990, Vol. 1, 752-756

[38] J. Reimann, R. Kirchner, N. Pfeff, D. Rackel, Tritium removal from NaK-cold traps, first results on hydride precipitation kinetics, Fusion Technology Vol. 21, (March 1992), 872-877

[39] J. Reimann, R. Kirchner, N. Pfeff, D. Rackel, Hydrogen removal from NaK with mesh-packed and meshless cold traps, Liquid Metal Systems, Karlsruhe, March 16-18 (1993)

[40] J. Reimann, R. Kirchner, N. Pfeff, D. Rackel, Tritium recovery from NaK-cold traps: investigation of hydrogen release kinetics, Fus.Eng. & Design 18 (1991), 67-72

[41] J. Reimann, R. Kirchner, N. Pfeff, D. Rackel, Tritium removal technique for a self-cooled Pb-17Li blanket, 18th SOFT, Karlsruhe, Aug. 22-26 (1994)

[42] K. Kleefeldt et al., KfK internal report (1993)

[43] T. Jordan, Kopplung der elektromagnetischen und strukturdynamischen Probleme beim Fusionsreaktorblanket, KfK 5236 (1993)

[44] J. Reimann et al., Convertible liquid metal blankets for ITER with Pb-17Li as breeding material, ISFNT-3, Los Angeles/USA (1994)

[45] F. Dammel, KfK internal report (1994)

[46] Siemens AG internal report (1992)

[47] W. Raskob, KfK, personal communication

[48] International Atomic Energy Agency, ITER Safety, ITER documentation series, No. 23, Vienna, 1991

[49] L. C. Cadwallader, S. J. Piet, 1988 Failure rate screening data for fusion reliability and risk analysis, EGG-FSP-7922, January 1988, Idaho National Engineering Laboratory

[50] H. John, H. Schnauder, E. Bogusch, J. Wehling, Reliability investigations and improvements of t he cooling system of a self-cooled liquid metal breeder blanket, 17th SOFT Rome, Italy, Fusion Technology 1992, Vol. 2, 1399-1403

[51] R. Bünde, S. Fabritssiev, V. Rybin, Reliability of welds and brazed joints in blankets and its influence on availability, Fusion Engineering and Design 16 (1991) 59-72, North-Holland

[52] H. Schnauder: Reliability analyses of the cooling systems of two DEMO breeder blanket concepts, 18th SOFT Karlsruhe 1994

[53] H. Glasbrenner, and H.U. Borgstedt, Preparation and characterization of Al_2O_3/Fe_xAl_y layers on MANET steel, J. Nucl. Mater. 212-215, p. 1561-1565 (1994)

[54] H.U. Borgstedt, H. Glasbrenner, and Z. Peric, Corrosion of insulating layers on MANET steel in flowing Pb-17Li, J. Nucl. Mater. 212-125, p. 1501-1503 (1994)

[55] H.U. Borgstedt, and H. Glasbrenner, The development of a direct insulation layer for liquid metal cooled fusion reactor blanket, accepted for publication in Fusion Eng. Des.

[56] E.R. Hodgson, Radiation enhanced electrical breakdown in fusion insulators from DC to 126 MHz, Journal of Nuclear Materials 191-194 (1992) 552-554

[57] A. Möslang, E. Dam, R. Lindau, Irradiation-induced electrical conductivities of AlN and Al_2O_3 at 450°C, 18th SOFT, Karlsruhe, 22 - 26 Aug., 1994

[58] S. Malang, H.U. Borgstedt, E.H. Farnum, K. Natesan, I.V. Vitkovski, Development of Insulating Coatings for Liquid Metal Blankets, ISFNT-3, Los Angeles, June 27 - July 1, 1994

[59] G. Schmitz, K. Schleisiek, H. John, KfK internal report (1993)

[60] S. Malang, P. Leroy, G.P. Casini, R.F. Mattas and Yu. Strebkov, Crucial Issues on liquid metal blanket design, Fusion Engng. Des. 16 (1991) pp. 95-109

Appendix: Main Characteristics of the Dual Coolant Blanket Concept

A) Neutronics

Breeding material	Pb-17Li enriched to 90 % ^{6}Li
Total tritium breeding ratio	1.15
Breeding ratio with 10 horizontal ports	1.09

Nuclear power generation [MW]
- outboard segment   26.7
- inboard segment   16.4

Afterheat generation [MW] in an outboard segment (2200 MW fusion power, 20000 h irradiation)

Time after shutdown	MANET	Pb-17Li	Total
0	0.208	0.527	0.735
10 s	0.207	7.73E-3	0.214
10 minutes	0.181	5.22E-3	0.186
1 hour	0.146	4.84E-3	0.151
1 day	1.99E-2	2.91E-3	2.28E-2
1 month	1.66E-2	1.87E-4	1.68E-2
1 year	7.09E-3	1.22E-4	7.21E-3
5 years	4.86E-4	9.41E-5	5.80E-4

B) Magnetohydrodynamics	outboard segment	inboard segment
Magnetic field strength [T]	5	7
Maximum liquid metal velocity [m/s]	1.1	0.4
MHD pressure drop [MPa]		
- with insulating coatings (reference case)	0.4	0.13
- with flow channel inserts (backup solution)	4.3	1.9

C) Thermohydraulics	outboard segment	inboard segment
First wall heat flux [MW/m^2]		
- maximum	0.5	0.5
- average	0.4	0.4
Max. power density [MW/m^3]		
- Manet	23.9	20.3
- Pb-17Li	19.4	17.1
Total Power (nuclear-power + surface heat flux) [MW]	30	19.6
Helium cooling:		
- power to be extracted [MW]	6.9	5.8
- pressure [MPa]	8	8
- temperature inlet/outlet [°C]	250/350	250/350
- mass flow rate [Kg/s]	13.2	5.55*
- max. velocity [m/s]	66	63
- pressure drop in segment [MPa]	0.15	0.12
- max. FW temperature [°C]	530	520
Liquid metal cooling:		
- power to be extracted [MW]	23.1	13.8
- temperature inlet/outlet [°C]	275/425	275/425
- mass flow rate [kg/s]	815	237*
- max. velocity [m/s]	1.1	0.4
- max. interface temperature (struct./breeder) [°C]	440	430

* for one blanket half

D) Mechanical stresses in outboard segment, calculated for average surface heat flux

Boundary conditions:

- internal pressure [MPa]	8
- FW surface heat load [MW/m^2]	0.4
- temperature of shield [°C]	285

Max. FW temperature [°C]	490

von Misses stresses [MPa]:

- primary membrane + bending	120
limit given by ASME	169
- primary + secondary	441
limit given by ASME	494

Max allowable internal pressure in the segment box during operation (estimated) [MPa]	11

E) Tritium control

Pb-17Li:

- max. tritium concentration [wppb]	1.2
- max. tritium partial pressure [Pa]	15
- total tritium inventory (in entire reactor) [g]	30

NaK:

- max. tritium concentration [wppb]	8
- max tritium partial pressure [Pa]	$2.3 \cdot 10^{-6}$
- min tritium concentration [wppb]	4
- min tritium partial pressure [Pa]	$0.6 \cdot 10^{-6}$
- total tritium inventory (in entire reactor, excluding cold traps) [g]	1
- max tritium inventory in one of the cold traps (2 recovery cycles per day) [g]	2.5

F) Steam generator design

Pb-17Li steam generators (SG):	outboard blanket	inboard blanket
power per unit (design value) [MW]	35	30
number of SG	48	32
type	double walled, straight tube	
tube diam. - outer tube OD/ID [mm] - inner tube OD/ID [mm]	30/26 24/20	
tube bundle height [m]	11	11
tube bundle diam. [m]	0.90	0.82
heat transfer area [m^2]	497	426

He steam generator (SG):	outboard blanket	inboard blanket
Power per unit (design value) [MW]	80	80
number of SG	6	4
type	single walled, helical coil	
tube diam. OD/ID [mm]	23/19	
tube length [m]	100	
tube bundle height [m]	7	
tube bundle diam. [m]	2.60	
heat transfer area [m^2]	2275	

G) Data used in safety analyses

Item	Unit	Outboard or Total	Inboard
Helium volume in first wall cooling system	m^3	855	537
Helium in FW cooling system			
in blanket segments	kg	888	184
in piping	kg	2270	1709
in circuit components	kg	2510	1672
Pb-17Li mass in blanket system			
in blanket segments	10^6 kg	3.1	0.9
in piping	10^6 kg	5.7	3.0
in circuit components	10^6 kg	8.2	4.2
Structural material			
in first wall (MANET)	10^3 kg	60	40
in breeding zone (MANET)	10^3 kg	800	500
in shield region (MANET)	10^3 kg	1000	800
in insulating layers (mainly Al)	10^3 kg	2.85	0.75
Tritium inventory			
in breeder material (Pb-17Li)	g	18	12
in FW coolant (helium)	g	0.15	
in intermediate coolant (NaK)	g	1	
in structural material (MANET)	g	19	
in recovery system	g	200	
Tritium permeation			
from Pb-17Li into helium	g/d	3	
from plasma into helium	g/d	1	
Partial pressure of HT in helium	Pa	0.18	
Tritium losses through steam generator			
from helium	Ci/d	10	
from NaK	Ci/d	10	
Energy stored in plasma	GJ	1000	
Work potential of helium	GJ	13	
Vacuum vessel volume	m^3	5000	
Delay time in shutdown after LOCA	s	1	
Surface heat flux			
average	W/cm^2	40	
peak value	W/cm^2	50	
Time to reduce surface heat flux to zero	s	20	